Supplementary Material: Correlation between supramolecular connectivity and magnetic behaviour of $[Fe^{III}(5\text{-}X\text{-}qsal)_2]^+$ based salts prone to exhibit SCO transition

Bruno J. C. Vieira [1,*], Laura C. J. Pereira [1,*], Vasco da Gama[1], Isabel C. Santos[1], Ana C. Cerdeira[1], João C. Waerenborgh[1]

[1] Centro de Ciências e Tecnologias Nucleares, DECN, Instituto Superior Técnico, Universidade de Lisboa, E.N. 10, km 139,7, 2695-066 Bobadela LRS, Portugal; brunovieira@ctn.tecnico.ulisboa.pt (B.J.C.V.); lpereira@ctn.tecnico.ulisboa.pt (L.C.J.P.); vascog@ctn.tecnico.ulisboa.pt (V.G.); icsantos@ctn.tecnico.ulisboa.pt (I.C.S.); acerdeira@ctn.tecnico.ulisboa.pt (A.C.C.); jcarlos@ctn.tecnico.ulisboa.pt (J.C.W.)

* Correspondence: brunovieira@ctn.tecnico.ulisboa.pt (B.J.C.V.); lpereira@ctn.tecnico.ulisboa.pt (L.C.J.P.)

Table S1 Summary of the crystal data, experimental details and refinement results

Table S2 Key parameters describing the DD contacts in the crystal structures of **3.BPh4** and **4.BPh4**, with the Dimer Chains supramolecular configuration.

Table S3 Key parameters describing the DD contacts in the crystal structures of the salts with type I Dimer Layers supramolecular configuration.

Table S4 Key parameters describing the DD contacts in the crystal structures of the salts with type II Dimer Layers supramolecular configuration.

Table S5 Key parameters describing the DD contacts in the crystal structures of **3.PF6.MeCN**, **4.PF6.H2O** and **5.PF6.2H2O**, with the Chain Layers supramolecular configuration.

Table S6 Summary of the parameters characterizing the SCO behavior of the salts with the Chain Layers supramolecular configuration and with HS configurations at room temperature.

Table S7 Summary of the parameters characterizing the octahedral distortion (Σ and θ).

Figure S1: Intrachain arrangements of the cations and DD contacts in the crystal structure of **4.BPh4**.

Figure S2: Top view of **4.BPh4** showing the most relevant DA contacts arrangement around one anion with cations from three neighbouring cationic chains. The cations in orange show ππ contacts to the Ph groups of the anion, those in light green show strong CH…π contacts to the anion and the ones depicted in light blue display weaker DA contacts.

Figure S3: View of the crystal structure of **3.Cl.MeCN.H2O** along *b*. The cations belonging to one of the cationic layers are depicted in dark blue.

Figure S4: Arrangement of the cations, anions and H_2O molecules within one layer of **3.Cl.MeCN.H2O** . The four cations in orange show ππ DD interactions with the central cationic dimer.

Figure S5: View of the interlayer DD contacts and arrangements of the $[Fe(5\text{-}X\text{-}qsal)_2]+$ cations relative to a central cation (in the default colour scheme) for **3.Cl.MeCN.H_2O** (a), **4.BF_4.H_2O** (b) and **3.ClO_4** (c). See text for details.

Figure S6: Indirect (D…X…D) connectivity mediated by one strongly coupled $Cl^{-}\cdots H_2O$ pair in **3.Cl.MeCN.H_2O**.

Figure S7: View of the crystal structure of **5.Cl.MeOH.3H_2O** along *c*. The cations belonging to one of the cationic layers are depicted in dark blue.

Figure S8: Arrangement of the cations within one layer of **5.Cl.MeOH.3H_2O**. The four cations in orange show strong ππ DD interactions with the central cationic dimer. The cations in darker orange correspond to cations with even stronger DD interactions, $DD^{iL}{}_1$, where the ππ interactions are reinforced by strong two fold CH…π interactions.

Figure S9: View of the DD contacts and arrangements of the $[Fe(5\text{-}I\text{-}qsal)_2]^+$ cations relative to a central cation (in the default colour scheme) for **5.Cl.MeOH.3H_2O**.

Figure S10: Indirect D…X…D connectivity in **5.Cl.MeOH.3H_2O** mediated by strongly coupled aggregates containing two Cl^- anions, six H_2O molecules and one methanol molecule with two possible locations. In one of those locations the MeOH atoms are depicted in light grey and its contacts are omitted.

Figure S11: View of the overlaps between the Ph-X groups in the DD interlayer interactions, DD^{iL}, in **5.Cl.MeOH.3H_2O** (a), **4.SCN.0.5H_2O** (b), **6.Cl.2MeOH.0.5H_2O** HS (c) and **6.Cl.2MeOH.0.5H_2O** LS (d).. View of the overlaps between the Ph-X groups in the DD interlayer interactions, DD^{iL}, in **5.Cl.MeOH.3H_2O** (a), **4.SCN.0.5H_2O** (b), **6.Cl.2MeOH.0.5H_2O** HS (c) and **6.Cl.2MeOH.0.5H_2O** LS (d).

Figure S12: Detail of the intrachain arrangement and the most relevant DD contacts in **5.PF_6.1.5H_2O**.

Figure S13: Arrangement of three cationic chains within one layer in **5.PF_6.1.5H_2O**. The cations in central chain are in the "ball and stick mode", while the cations of the other two are represented in the "stick mode". The cations in orange displays strong ππ interactions with cations from the central chain further reinforced by two fold CH…π interactions.

Figure S14: View in the default colour scheme of the interlayer DD contacts and arrangements of the $[Fe(5\text{-}I\text{-}qsal)_2]^+$ cations relative to a central cation for **5.PF_6.1.5H_2O**. Only the cations depicted in light blue and in violet belong to the neighbouring layers, those in light grey and orange are located in the same layer as the central cations (the contacts involving these cations are omitted for clarity).

Figure S15: Indirect (D…A…D) connectivity mediated by one PF_6^- anion in **5.PF_6.1.5H_2O**. The anion shows interactions to four cations (D1-D4) in one layer and to another cation (D5) located in a neighbouring layer.

Figure S16: Indirect connectivity assistance to the direct DD intrachain, (a) $DD^{Ch}{}_1$ and (b) $DD^{Ch}{}_2$, intralayer (c) DD^{L} and interlayer (d) $DD^{iL}{}_1$ interactions in **5.PF_6.1.5H_2O**. $DD^{Ch}{}_1$ is assisted by a pair of interactions mediated by the H_2O molecules and for $DD^{Ch}{}_2$, DD^{L} and $DD^{iL}{}_1$ the DD interactions are assisted by a pair of DAD connections.

Figure S17: Intrachain indirect connectivity mediated by the solvent molecules and anions to the direct DD interactions (DD^{Ch}_1 and DD^{Ch}_2) in **3.PF$_6$.MeCN** (a and d), **4.PF$_6$.H$_2$O** (b and e) and **5.PF$_6$.1.5H$_2$O** (c and f).

Figure S18: Indirect DAD connectivity assistance to the direct DD intralayer (DD^{L}) and interlayer (DD^{iL}_1 and DD^{iL}_2) interactions regarding **3.PF$_6$.MeCN** (a, d and g), **4.PF$_6$.H$_2$O** (b e and h) and **5.PF$_6$.1.5H$_2$O** (c, f and i).

Table S1. Summary of the crystal data, experimental details and refinement results

	3.Cl.MeCN.H_2O	**3.ClO_4**	**3.PF_6.MeCN**	**3.BF_4**
Empirical Formula	C_{34} H_{25} Cl_3 Fe N_5 O_3	C_{32} H_{20} Cl_3 Fe N_4 O_6	C_{34} H_{23} Cl_2 F_6 Fe N_5 O_2 P	C_{34} H_{23} B Cl_2 F_4 Fe N_5 O_2
Molecular mass	713.79	718.72	805.29	747.13
Temperature	150(2) K	150(2) K	150(2)	293(2) K
Crystal size (mm)	0.220 x 0.180 x 0.100	0.200 x 0.100 x 0.080	0.200 x 0.140 x 0.050	0.400x0.100x0.050
Crystal colour, shape	Black, prism	Black, prism	Black, prism	Black, prism
Crystal system	Monoclinic	Triclinic	Triclinic	Triclinic
Space group (no.)	P 21/n	P-1	P-1	P-1
a (Å)	12.2867(4)	10.0903(2)	11.6572(5)	11.6278(4)
b (Å)	15.2146(6)	12.4912(3)	12.4883(6)	12.3036(4)
c (Å)	16.2029(6)	23.0761(7)	12.7109(6)	12.5792(4)
α (Å)	90	86.2860(10)	109.7630(10)	69.491(2)
β (Å)	92.3130(10)	80.0800(10)	90.3900(10)	69.337(2)
γ (Å)	90	89.925(2)	111.8440(10)	88.467(2)
V (Å3)	3026.46(19)	2858.87(12)	1597.67(13)	1567.47(9)
Z, Dcalcd. (mg m^{-3})	4, 1.567	4, 1.670	2, 1.674	2, 1.583
μ (mm^{-1})	0.81	0.864	0.768	0.718
F(000)	1460	1460	814	758
Theta range (deg)	2.959 to 26.372	2.917 to 25.029	2.755 to 25.027	2.730 to 25.678
Index range (h, k, l)	-15/15,-19/18, -20/19	-12/12,-14/14,-27/27	-11/13,-14/14,-15/15	-14/13,-14/14,-15/14
Refl. collected/unique	23199/6121[Rint=0.0401]	24611/10013[Rint=0.0529]	9327/5536 [Rint=0.0343]	14524/5849[Rint=0.0372]
Completeness θ =25.242	99.20%	99.40%	98.00%	98.40%
T max./min.	0.923 and 0.842	0.934 and 0.846	0.963 and 0.862	0.965 and 0.762
Goodness-of-fit on F2	1.042	1.007	1.051	1.059
Final R1 [I > 2σ(I)]/wR2	R1 = 0.0341, wR2 = 0.0782	R1=0.0489, wR2=0.1086	R1=0.0413, wR2=0.0910	R1 = 0.0482, wR2 = 0.1185
Spin State	Low-Spin	Low-Spin	Low-Spin (SCO)	Low-Spin
Supramolecular Configuration	Type I Dimer Layers	Type I Dimer Layers	Chain Layers	Type I Dimer Layers

Table S1 (continued)

	3.BPh_4	**4.Cl.MeCN.H_2O**	**4.ClO_4**	**4.PF_6.H_2O**
Empirical Formula	C_{56} H_{40} B Cl_2 Fe N_4 O_2	C_{34} H_{25} Cl Br_2 Fe N_5 O_3	C_{32} H_{20} Cl Br_2 Fe N_4 O_6	C_{32} H_{22} Br_2 F_6 Fe N_4 O_3 P
Molecular mass	938.48	802.71	807.64	871.17
Temperature	150(2) K	150(2) K	150(2) K	150(2)
Crystal size (mm)	0.260 x 0.160 x 0.030	0.350 x 0.200 x 0.100	0.100 x 0.080 x 0.060	0.200 x 0.100 x 0.060
Crystal colour, shape	Black, prism	Black, prism	Black, prism	Black, prism
Crystal system	Triclinic	Monoclinic	Triclinic	Triclinic
Space group (no.)	P-1	P 21/n	P-1	P-1
a (Å)	11.5300(3)	12.2907(5)	10.2637(5)	11.9483(3)
b (Å)	14.1235(5)	15.3389(6)	12.4457(5)	12.4436(4)
c (Å)	14.5540(5)	16.4190(7)	23.3685(12)	12.4841(3)
α (Å)	84.5220(10)	90	87.405(2)	67.9420(10)
β (Å)	86.360(2)	91.8110(10)	78.898(2)	87.698(2)
γ (Å)	71.6650(10)	90	89.622(3)	70.081(2)
V (Å3)	2238.03(13)	3093.9(2)	2926.2(2)	1609.13(8)
Z, Dcalcd. (mg m^{-3})	2, 1.393	4, 1.723	4, 1.833	2,1.798
μ (mm^{-1})	0.506	3.202	3.393	3.078
F(000)	970	1604	1604	862
Theta range (deg)	2.748 to 25.681	2.815 to 25.027	3.193 to 25.026	2.665 to 25.681
Index range (h, k, l)	-14/14, -17/17, -17/17	-14/14,-18/18, -19/19	-12/11,-14/14,-27/27	-14/13,-14/15,-14/15
Refl. collected/unique	22508/8433[Rint=0.0386]	37478/5461[Rint=0.0477]	21145/10261[Rint=0.0678]	13003/6064 [Rint=0.0425]
Completeness θ =25.242	99.30%	99.80%	99.40%	99.4
T max./min.	0.985 and 0.880	0.740 and 0.400	0.822 and 0.728	0.837 and 0.578
Goodness-of-fit on F2	1.039	1.091	0.887	0.964
Final R1 [I > 2σ(I)]/wR2	R1=0.0408, wR2 = 0.0933	R1 = 0.0349, wR2 = 0.0863	R1=0.0559, wR2=0.0939	R1=0.0464, wR2=0.1094
Spin State	Low-Spin	Low-Spin	Low-Spin	Low-Spin (SCO)
Supramolecular Configuration	Dimer Chains	Type I Dimer Layers	Type I Dimer Layers	Chain Layers

Table S1 (continued)

	4.SCN.0.5H_2O	**4.BF_4.0.5H_2O**	**4.BPh_4**	**5.Cl.MeOH.2.5H_2O**
Empirical Formula	C_{66} H_{42} Br_4 Fe_2 S_2 N_{10} O_5	$C_{64}H_{42}B2Br_4F_8Fe_2N_8O_5$	C_{56} H_{40} B Br_2 Fe N_4 O_2	C_{65} H_{52} Cl_2 Fe_2 I_4 N_8 O_{11}
Molecular mass	1550.55	1608.01	1027.4	1811.34
Temperature	150(2) K	150(2) K	150(2) K	150(2) K
Crystal size (mm)	0.200x0.160x0.100	0.350x0.200x0.060	0.240 x 0.200 x 0.130	0.160 x 0.060 x 0.020
Crystal colour, shape	Black, prism	Black, prism	Black, prism	Black, prism
Crystal system	Triclinic	Monoclinic	Triclinic	Triclinic
Space group (no.)	P-1	P 21/n	P-1	P-1
a (Å)	11.0587(6)	13.5594(8)	11.6596(2)	10.7546(7)
b (Å)	12.3463(7)	16.0511(9)	14.2408(3)	12.6720(8)
c (Å)	12.5416(8)	14.3784(9)	14.5222(3)	13.9877(10)
α (Å)	63.4200(10)	90	85.0640(10)	63.558(2)
β (Å)	74.087(2)	106.775(2)	85.9370(10)	74.536(2)
γ (Å)	73.265(2)	90	70.4880(10)	74.864(2)
V (Å3)	1560.48(16)	2996.2(3)	2262.11(8)	1622.52(19)
Z, Dcalcd. (mg m^{-3})	1, 1.650	2, 1.782	2, 1.508	1, 1.854
μ (mm^{-1})	3.152	3.237	2.149	2.499
F(000)	772	1592	1042	884
Theta range (deg)	2.959 to 25.026	2.938 to 25.346	2.995 to 25.026 deg.	2.910 to 25.027
Index range (h, k, l)	-12/13,-14/14,-16/14	-13/16,-19/18,-17/17	-13/13, -16/16, -17/17	-12/12,-15/12,-16/16
Refl. collected/unique	9125/5405[Rint=0.0233]	20689/5486[Rint=0.0632]	42720/7940[Rint=0.0323]	11554/5638 [Rint= 0.0447]
Completeness θ =25.242	98.00%	99.9	99.50%	98.30%
T max./min.	0.743 and 0.571	0.829 and 0.397	0.768 and 0.627	0.952 and 0.691
Goodness-of-fit on F2	1.072	1.109	1.084	1.061
Final R1 [I > 2σ(I)]/wR2	R1 = 0.0417, wR2 = 0.1100	R1=0.0577, wR2= 0.1541	R1=0.0280, wR2 = 0.0672	R1 = 0.0450, wR2 = 0.1252
Spin State	High-Spin	Low-Spin	Low-Spin	High-Spin
Supramolecular Configuration	Type II Dimer Layers	Type I Dimer Layers	Dimer Chains	Type II Dimer Layers

Table S1 (continued)

	5.PF_6.1.5H_2O
Empirical Formula	C_{64} H_{46} I_4 F_{12} Fe_2 N_8 O_7 P_2
Molecular mass	1948.34
Temperature	150(2)
Crystal size (mm)	0.200 x 0.020 x 0.020
Crystal colour, shape	Black, prism
Crystal system	Triclinic
Space group (no.)	P-1
a (Å)	12.3301(4)
b (Å)	12.4309(5)
c (Å)	12.5360(5)
α (Å)	87.794(2)
β (Å)	68.4950(10)
γ (Å)	68.6750(10)
V (Å3)	1655.29(11)
Z, Dcalcd. (mg m^{-3})	1, 1.955
μ (mm^{-1})	2.446
F(000)	944
Theta range (deg)	3.035 to 25.023
Index range (h, k, l)	-14/14,-14/13,-14/14
Refl. collected/unique	15989/5613 [Rint=0.0501]
Completeness θ =25.242	95.8
T max./min.	0.953 and 0.640
Goodness-of-fit on F2	1.041
Final R1 [I > 2σ(I)]/wR2	R1=0.0398, wR2=0.0721
Spin State	Low-Spin (SCO)
Supramolecular Configuration	Chain Layers

Table S2. Key parameters describing the DD contacts in the crystal structures of **3.BPh4** and **4.BPh4**, with the Dimer Chains supramolecular configuration

	3.BPh$_4$ (150K)					**4.BPh$_4$ (150K)**				
	LS					**LS**				
Dimer	**d**	**α**	**ov**	**comm.**		**d**	**α**	**ov**	**comm.**	
[D…D]										
DD^d	**3.417**	**0**	**(L-L)^{II}/0.3**	**ππ**		**3.462**	**0**	**(L-L)^{II}/0.3**	**ππ**	
	2.576	**152.1**	**----**	**C-H…O^{2F}**		**2.603**	**152.2**	**----**	**C-H…O^{2F}**	
	3.397	**80.1**	**----**	**C-Cl…π^{2F}**	**D…D**	**3.502**	**88.7**	**----**	**C-Br…π^{2F}**	**D…D**
Chain	**d**	**α**	**ov**	**comm.**		**d**	**α**	**ov**	**comm.**	
DD…DD										
DD^{Ch}	**3.427**	**128.3**	**----**	**C-Cl…π**	**D…D**	**3.479**	**124.4**	**----**	**C-Br…π**	**D…D**

[a], DD interactions within the dimers (DD^d) and interdimer intrachain (DD^{Ch})

d, interatomic separation of the contacts or distance between the average planes of the ligands in the case of ππ interactions.

α, angle of the contact or angle between the average planes in the case of ππ interactions.

overlap, characterization of the ππ overlap.

L-L corresponds to the overlap over the entire length of the ligand (with two overlaps between the Ph and Qn groups).

The index $^{I/II}$ refers to the number of overlapping rings.

The numerical value corresponds to an estimation of the extension of the overlap (as the fraction of the area of the overlap vs. the area of one ring)

contact, characterization of the contact (the superscript 2F concerns two fold contacts)

Int. cat., interacting cations

Colour Code: Red corresponds to ππ interactions, Blue corresponds to hydrogen bonds, Purple corresponds to halogen bonds.

Table S3. Key parameters describing the DD contacts in the crystal structures of the salts with type I Dimer Layers supramolecular configuration (continues next page)

[a]	3.Cl.MeCN.H2O (150K)					4.Cl.MeCN.H2O (150K)					4BF4.H2O (150K)				
	LS					LS					LS				
Dimer	*d* (Å)	*α* (°)	overlap	contact	Int. cat.	*d* (Å)	*α* (°)	overlap	contact	Int. cat.	*d* (Å)	*α* (°)	overlap	contact	Int. cat.
DD^{d}	3.403	0	$(L\text{-}L)^{II}/0.3$	ππ		3.410	0	$(L\text{-}L)^{II}/0.3$	ππ		*3.352*	0	$(L\text{-}L)^{II}/0.5$	ππ	
	2.478	150.7	----	$C\text{-}H\cdots O^{2F}$		2.456	151.9	----	$C\text{-}H\cdots O^{2F}$		2.652	152.9	----	$C\text{-}H\cdots O^{2F}$	D...D
	3.525*	87.4	----	$C\text{-}Cl\cdots\pi^{2F}$	D...D	3.574	86.1	----	$C\text{-}Br\cdots\pi^{2F}$	D...D	3.492	102.9	----	$C\text{-}Br\cdots\pi^{2F}$	
Layer															
DD^{L}	3.379	2.3	(Ph-Qn)/0	ππ		3.400	3.8	(Ph-Qn)/0	ππ		3.382	11.0	(Ph-Qn)/0	ππ	
2 x DD^{L}	3.630*	88.3	----	$C\text{-}Cl\cdots\pi$	D...D	3.686*	69.3	----	$C\text{-}Br\cdots\pi$	D...D	3.738*	83.3	----	$C\text{-}Br\cdots\pi$	D...D
interLayer															
$DD^{iL}{}_{1}$			no overlap					no overlap			3.568	0	(Ph-Ph)/0	ππ	
	2.927	158.9	----	$C\text{-}Cl\cdots H^{2F}$	D...D	2.956	160.9	----	$C\text{-}Br\cdots H^{2F}$	D...D	2.986	160.5	----	$C\text{-}Br\cdots H^{2F}$	D...D
$DD^{iL}{}_{2}$	3.370	35.1	no overla	C...C		3.378	35.9	no overla	C...C		3.711*	45.5	no overla	C...C	
2 x $DD^{iL}{}_{2}$	3.297	125.5	----	$C\text{-}Cl\cdots\pi$	D...D	3.372	124.5	----	$C\text{-}Br\cdots\pi$	D...D	2.642	150.3	----	$C\text{-}H\cdots\pi$	D...D

[a], DD interactions within the dimers (DD^{d} or $DD^{d}{}_{X}$), the layers (DD^{L} or $DD^{L}{}_{X}$) and interlayer (DD^{iL} or $DD^{iL}{}_{X}$)

d, interatomic separation of the contacts or distance between the average planes of the ligands in the case of ππ interactions

α, angle of the contact or angle between the average planes (in the case of ππ interactions)

overlap, characterization of the ππ overlap.

L-L corresponds to the overlap over the entire length of the ligand (with two overlaps between the Ph and Qn groups). **Qn-Qn** overlap of two Qn groups; **Ph-Ph** overlap beween two Ph groups and **Ph-Qn** overlap between a Ph and Qn.

The index $^{I/II}$ refers to the number of overlapping rings. Only observed in the case of L-L or Qn-Qn. In the case of the contacts involving the Ph groups only one ring may overlap.

The numerical value corresponds to an estimation of the extension of the overlap (as the fraction of the area of the overlap vs. the area of one ring)

contact, characterization of the contact (the superscript 2F concerns two fold contacts)

Int. cat., interacting cations

*slightly elongated contacts, exceeding the sum of the van der Waals radii by 2%, or 5% in case of ππ contacts

Colour Code: Red corresponds to ππ interactions, Blue corresponds to hydrogen bonds, Purple corresponds to halogen bonds.

Table S3. continued

	3.BF4 (150K) LS					3.ClO4 (150K) LS					4.ClO4 (150K) LS				
Dimer	*d* (Å)	*α* (°)	overlap	contact	Int. cat.	*d* (Å)	*α* (°)	overlap	type	Int. cat.	*d* (Å)	*α* (°)	overlap	contact	Int. cat.
DD^{d}_{A}	3.330	0	$(L\text{-}L)^{II}/0.5$	ππ		3.354	0	$(L\text{-}L)^{II}/0.5$	ππ		3.301	0	$(L\text{-}L)^{II}/0.5$	ππ	
	2.777*	150.7	----	C-H…O^{2F}		2.750	144.1	----	C-H…O^{2F}		2.736	141.9	----	C-H…O^{2F}	
	3.349	81.4	----	C-Cl…π^{2F}	$D_A…D_A$	3.336	82.8	----	C-Cl…π^{2F}	$D_A…D_A$	3.434	101.7	----	C-Br…π^{2F}	$D_A…D_A$
DD^{d}_{B}	3.537	0	$(L\text{-}L)^{II}/0.1$	ππ	$D_B…D_B$	3.482	0	$(L\text{-}L)^{II}/0.1$	ππ	$D_B…D_B$	3.545	0	$(L\text{-}L)^{II}/0.1$	ππ	$D_B…D_B$
Layer															
DD^{L}_{1}	3.498	8.4	(Ph-Qn)/0	ππ		3.476	8.2	(Ph-Qn)/0	ππ		3.480	9.5	(Ph-Qn)/0	ππ	
	3.530*	104.9	----	C-Cl…π	$D_A…D_B$	3.604*	104.1	----	C-Cl…π	$D_A…D_B$	3.654*	89.5	102.1	C-Br…π	$D_A…D_B$
DD^{L}_{2}	3.483	5.3	(Ph-Qn)/0	ππ		3.493	4.9	(Ph-Qn)/0	ππ		3.413	6.3	(Ph-Qn)/0	ππ	
	2.930	146.3	----	C-H…π		3.038*	145.6	----	C-H…π		3.082*	143.0	----	C-H…π	
	2.949	158.2	----	C-H…π	$D_A…D_B$	2.985*	157.4	----	C-H…π	$D_A…D_B$	3.015*	159.4	----	C-H…π	$D_A…D_B$
interLayer															
DD^{iL}_{1}	3.267	0	(Ph-Ph)/0	ππ		3.255	0	(Ph-Ph)/0	ππ		3.267	0	(Ph-Ph)/0	ππ	
	3.259	138.8	----	C-Cl…π^{2F}	$D_A…D_A$	3.257	137.0	----	C-Cl…π^{2F}	$D_A…D_A$	3.350	135.5	----	C-Br…π^{2F}	$D_A…D_A$
DD^{iL}_{2}	3.382	4.4	(Ph-Ph)/0	ππ		3.388	4.4	(Ph-Ph)/0	ππ		3.470	3.4	(Ph-Ph)/0	ππ	
	3.445	90.8	----	C-Cl…π	$D_A…D_B$	3.462	83.5	----	C-Cl…π	$D_A…D_B$	3.519	91.1	----	C-Br…π	$D_A…D_B$
DD^{iL}_{3}	3.614*	0	(Ph-Ph)/0	ππ		3.833*	0	(Ph-Ph)/0	ππ		3.627*	0	(Ph-Ph)/0	ππ	
	3.279	134.7	----	C-Cl…π^{2F}	$D_B…D_B$	3.335	129.8	----	C-Cl…π^{2F}	$D_B…D_B$	3.374	131.8	----	C-Br…π^{2F}	$D_B…D_B$
DD^{iL}_{4}	3.632*	0	$(Qn\text{-}Qn)^{I}/$	ππ	$D_B…D_B$	3.599*	0	$(Qn\text{-}Qn)^{I}/$	ππ	$D_B…D_B$	3.596*	0	$(Qn\text{-}Qn)^{I}/$	ππ	$D_B…D_B$

[a], DD interactions within the dimers (DD^{d} or DD^{d}_{X}), the layers (DD^{L} or DD^{L}_{X}) and interlayer (DD^{iL} or DD^{iL}_{X})

d, interatomic separation of the contacts or distance between the average planes of the ligands (in the case of ππ interactions)

α, angle of the contact or angle between the average planes (in the case of ππ interactions)

overlap, characterization of the ππ overlap.

L-L corresponds to the overlap over the entire length of the ligand (with two overlaps between the Ph and Qn groups). **Qn-Qn** overlap of two Qn groups; **Ph-Ph** overlap beween two Ph groups and **Ph-Qn** overlap between a Ph and Qn.

The index $^{I/II}$ refers to the number of overlapping rings. Only observed in the case of L-L or Qn-Qn. In the case of the contacts involving the Ph groups only one ring may overlap.

The numerical value corresponds to an estimation of the extension of the overlap (as the fraction of the area of the overlap vs. the area of one ring)

contact, characterization of the contact (the superscript 2F concerns two fold contacts)

Int. cat., interacting cations

*slightly elongated contacts, exceeding the sum of the van der Waals radii by 2%, or 5% in case of ππ contacts

Colour Code: Red corresponds to ππ interactions, Blue corresponds to hydrogen bonds, Purple corresponds to halogen bonds.

Table S4. Key parameters describing the DD contacts in the crystal structures of the salts with type II Dimer Layers supramolecular configuration.

[a]	4.SCN.2H$_2$O (150K)					5.Cl.MeOH.3H$_2$O (150K)				
	HS					HS				
Dimer	***d*** **(Å)**	***α*** **(°)**	**overlap**	**contact**	**Int. cat.**	***d*** **(Å)**	***α*** **(°)**	**overlap**	**contact**	**Int. cat.**
DD^{d}	3.549	0	(L-L)^{II}/0.7	ππ		3.459	0	(L-L)^{II}/0.5	ππ	
	2.622	146.8	----	C-H…O^{2F}		2.625	152.0	----	C-H…O^{2F}	D…D
	2.692	142.6	----	C-H…O^{2F}	D…D					
Layer										
DD$^{L}_{1}$	3.377	0	(Qn-Qn)^{II}	ππ		3.426	0	(Qn-Qn)^{II}	ππ	
	2.799	159.7	----	C-H…π^{2F}		2.720	157.3	----	C-H…π^{2F}	
	2.717	167.1	----	C-H…π^{2F}	D…D	2.944	154.2	----	C-H…π^{2F}	D…D
DD$^{L}_{2}$	3.392	0	(Qn-Qn)^{II}	ππ	D…D	3.424	0	(Qn-Qn)^{II}	ππ	D…D
interLayer										
DD^{iL}	3.502	0	(Ph-Ph)/(	ππ		3.581*	0	(Ph-Ph)/(	ππ	
	3.113	155.0	----	C-Br…O^{2F}	D…D	3.243	151.5	----	C-I…O^{2F}	D…D

[a], DD interactions within the dimers (DD^{d} or DD^{d}$_{X}$), the layers (DD^{L} or DD^{L}$_{X}$) and interlayer (DD^{iL} or DD^{iL}$_{X}$)

d, interatomic separation of the contacts or distance between the average planes of the ligands in the case of ππ interactions

α, angle of the contact or angle between the average planes in the case of ππ interactions.

overlap, characterization of the ππ overlap.

L-L corresponds to the overlap over the entire length of the ligand (with two overlaps between the Ph and Qn groups).

Qn-Qn overlap of two Qn groups; **Ph-Ph** overlap beween two Ph groups and **Ph-Qn** overlap between a Ph and Qn.

The index $^{I/II}$ refers to the number of overlapping rings. Only observed in the case of L-L or Qn-Qn. In the case of the contacts involving the Ph groups only one ring may overlap.

The numerical value corresponds to an estimation of the extension of the overlap (as the fraction of the area of the overlap vs. the area of one ring)

contact, characterization of the contact (the superscript 2F concerns two fold contacts)

Int. cat., interacting cations

*slightly elongated contacts, exceeding the sum of the van der Waals radii by 2%, or 5% in case of ππ contacts

Colour Code: Red corresponds to ππ interactions, Blue corresponds to hydrogen bonds, Purple corresponds to halogen bonds.

Table S5. Key parameters describing the DD contacts in the crystal structures of **3.PF$_6$.MeCN**, **4.PF$_6$.H$_2$O** and **5.PF$_6$.2H$_2$O**, with the Chain Layers supramolecular configuration

[a]	3.PF6.MeCN (150K)					4.PF6.H$_2$O (150K)					5.PF6.1.5H$_2$O (150K)				
	LS	Tc=265K	Sharp			LS	Tc=220K	~ Sharp			LS	Tc=270K	V. Sharp		
Chain	***d*** **(Å)**	***α*** **(º)**	**overlap**	**contact**	**Int. cat.**	***d*** **(Å)**	***α*** **(º)**	**overlap**	**contact**	**Int. cat.**	***d*** **(Å)**	***α*** **(º)**	**overlap**	**contact**	**Int. cat.**
DD$^{Ch}_1$	3.322	0	(L-L)^{II}/0.5	ππ		3.318	0	(L-L)^{II}/0.5	ππ		3.322	0	(L-L)^{II}/0.5	ππ	
	2.624	148.3	----	C-H…O^{2F}		2.526	150.6	----	C-H…O^{2F}		2.493	150.4	----	C-H…O^{2F}	
	3.516	77.1	----	C-Cl…π^{2F}	D…D	3.590	91.9	----	C-Br…π^{2F}	D…D	3.700	88.2	----	C-I…π^{2F}	D…D
DD$^{Ch}_2$	3.504	0	(L-L)^{II}/0.5	ππ		3.441	0	(L-L)^{II}/0.5	ππ		3.449	0	(L-L)^{II}/0.5	ππ	
	2.680	147.8	----	C-H…O^{2F}		2.741	148.4	----	C-H…O^{2F}		2.738	147.1	----	C-H…O^{2F}	
	3.431	83.4	----	C-Cl…π^{2F}	D…D	3.579	99.6	----	C-Br…π^{2F}	D…D	3.657	94.7	----	C-I…π^{2F}	D…D
Layer															
DD^{L}	3.445	0	(Qn-Qn)^{I}/	ππ		3.380	0	(Qn-Qn)^{I}/	ππ		3.350	0	(Qn-Qn)^{I}/	ππ	
	2.799	150.4	----	C-H…π^{2F}	D…D	2.779	162.2	----	C-H…π^{2F}	D…D	2.796	145.0	----	C-H…π^{2F}	D…D
interLayer															
DD$^{iL}_1$	3.075*	152.5	----	C-H…Cl^{2F}		3.131*	159.2	----	C-H…Br^{2F}		3.192	157.0	----	C-H…I^{2F}	
	2.855	137.2	----	C-H…π^{2F}	D…D	3.038*	143.6	----	C-H…π^{2F}	D…D	3.154*	141.6		C-H…π^{2F}	D…D
DD$^{iL}_2$	3.618*	128.3	----	C-Cl…π		3.405	134.0	----	C-Br…π		3.554	138.0	----	C-I…π	
2 x DD$^{iL}_2$	3.646*	111.2	----	C-Cl…π	D…D	3.676*	113.3	----	C-Br…π	D…D	3.817*	120.5	----	C-I…π	D…D

[a], DD interactions within the chains (DD$^{Ch}_X$), the layers (DD^{L}) and interlayer (DD^{iL} or DD$^{iL}_X$)

d, interatomic separation of the contacts or distance between the average planes of the ligands in the case of ππ interactions

α, angle of the contact or angle between the average planes in the case of ππ interactions.

overlap, characterization of the ππ overlap.

L-L corresponds to the overlap over the entire length of the ligand (with two overlaps between the Ph and Qn groups).

Qn-Qn overlap of two Qn groups.

The index $^{I/II}$ refers to the number of overlapping rings. Only observed in the case of L-L or Qn-Qn. In the case of the contacts involving the Ph groups only one ring may overlap.

The numerical value corresponds to an estimation of the extension of the overlap (as the fraction of the area of the overlap vs. the area of one ring)

contact, characterization of the contact (the superscript 2F concerns two fold contacts)

Int. cat., interacting cations

*slightly elongated contacts, exceeding the sum of the van der Waals radii by 2%, or 5% in case of ππ contacts

Colour Code: Red corresponds to ππ interactions, Blue corresponds to hydrogen bonds, Purple corresponds to halogen bonds.

Table S6. Summary of the parameters characterizing the SCO behavior of the salts with the Chain Layers supramolecular configuration and with HS configurations at room temperature.

Salt	RT config	Int. config.	LT config.	χT_{RT} (emu/mol.K)	SCO Steps	SCO type$	$T_{1/2}^1$ (K) $T_{1/2}^2$ (K)	Ref
1.[Fe(CN)$_5$(CO)]MeOH	HS	…	LS	4.1	1 Step	g (95K)	122	X13
	HS	…	HS		…	Blocked	…	…
1.I$_3$	HS	…	LS	3.7	1 Step	g/Sh (69K)	240	X15
1.SCN	HS	HS (33%)	LS	4.1	2 Step	Sh (25K)	203$^{\downarrow}$, 290$^{\uparrow}$	X17
	HS	LS (67%)	LS			Sh (25K)	203$^{\downarrow}$, 210$^{\uparrow}$	
1.SeCN	HS	HS (33%)	LS	4.2	2 Step	VSh (10K)	212$^{\downarrow}$, 282$^{\uparrow}$	X30
	HS	LS (67%)	LS			VSh (10K)	212$^{\downarrow}$, 215$^{\uparrow}$	
3.SCN.MeOH	HS	HS (50%)	LS	3.2	2 step	g/Sh (73K)	250	X18
	HS	LS (50%)	LS			Sh (40K)	167$^{\downarrow}$, 177$^{\uparrow}$	
3.PF$_6$.MeCN	HS	…	LS	3.8	1 Step	Sh (44K)	265	this work
4.NO$_3$.2MeOH	HS	HS (50%)	LS	4.1	2 Step	VSh (13K)	229$^{\downarrow}$, 234$^{\uparrow}$	X19
	HS	LS (50%)	LS			VSh (12K)	128$^{\downarrow}$, 144$^{\uparrow}$	
4.PF$_6$.H$_2$O	HS	…	LS	3.6	1 Step	g/Sh (60K)	220	this work
5.CF$_3$SO$_3$.nPrOH	HS	…	LS	4.1	1 Step	g/Sh (64K)	199	X20
5.CF$_3$SO$_3$.iPOH	HS	…	LS	3.7	1 Step	g (96K)	251	X20
5.CF$_3$SO$_3$.MeOH	HS	…	LS	4.2	1 Step	VSh (8K)	232$^{\downarrow}$, 234$^{\uparrow}$	X21
5.CF$_3$SO$_3$.EtOH	HS	…	LS	4.2	…	Irrev.	…	X20
5.PF$_6$.1.5H$_2$O	HS	…	LS	4.2	1 Step	VSh (4K)	268$^{\downarrow}$, 272$^{\uparrow}$	this work
5.N(SO$_2$CF$_3$)$_2$	HS	…	LS	4.2	1 Step	VSh (7K)	244$^{\downarrow}$, 278$^{\uparrow}$	X31
6.Cl.MeCN.H$_2$O	HS	HS (50%)	LS	4.2	2 Step	Sh (21K)	270	X12
	HS	LS (50%)	LS			VSh (12K)	240	
7.Cl.4MeOH. H$_2$O	HS	…	HS	4.1	…	Blocked	…	X28
7.ClO$_4$.MeOH	HS	…	HS	3.7	…	Blocked	…	X28
7.NO$_3$	HS	…	HS	4.2	…	Blocked	…	X28

$T_{1/2}^1$ and $T_{1/2}^2$ are the $T_{1/2}$ observed when T decreases $^{\downarrow}$ and when T increases $^{\uparrow}$, when there is hysteresis.

$ type of transition and degree of cooperativity (g-gradual, g/Sh-gradual/Sharp, Sh-Sharp and VSh-Very Sharp).

The value between brackets (ΔT^*, in K) corresponds to the estimated span of the HS→LS transition. considering the slope of $d\chi T/dT$ at $T_{1/2}$ and extrapolating it to the χT^{HS} and χT^{LS} limits.

Increasing degree of cooperativity: g (for ΔT^*>90K); g/Sh (50<ΔT^*<90K); Sh (15<ΔT^*<50); VSh (ΔT^*<15).

There are two ΔT values, $\Delta T_{1/2}^1$ (K), $\Delta T_{1/2}^2$ (K), when SCO takes place in two steps.

Blocked HS configuration; Irrev. Irreversible SCO processes.

Table S7 Summary of the parameters characterizing the octahedral distortion (Σ and θ).

Compound	Σ(°)	θ(°)	Spin State	Supramolecular Configuration
3.Cl.MeCN.H_2O	42.08	63.13	LS	Dimer Layers I
3.ClO_4	42.54	61.01	LS	Dimer Layers I
	53.38	72.8		
3.BF_4	40.37	56.74	LS	Dimer Layers I
	52.65	72.41		
3.PF_6.MeCN	42.14	61.61	LS (SCO)	Chain Layers
3.BPh_4	45.17	64.36	LS	Dimer Chains
4.Cl.MeCN.H_2O	44.18	65.52	LS	Dimer Layers I
4.ClO_4	40.37	56.74	LS	Dimer Layers I
	53.48	72.18		Dimer Layers I
4.BF_4.0.5H_2O	49.8	80.8	LS	Dimer Layers I
4.PF_6.H_2O	43.87	61.32	LS (SCO)	Chain Layers
4.BPh_4	42.59	60.94	LS	Dimer Chains
4.SCN.0.5H_2O	65.62	218	HS	Dimer Layers II
5.Cl.MeOH.2.5H_2O	71.27	209	HS	Dimer Layers II
5.PF_6.1.5H_2O	45.37	63.89	LS (SCO)	Chain Layers

Σ quantifies the angular deviation from an ideal octahedral geometry and θ indicates the distortion from an octahedral towards a trigonal prismatic geometry, both indexes being 0 for an ideal octahedron. Colour code according to the supramolecular configuration: Blue – Type I Dimer layer, Orange – Chain Layers, Purple – Dimer Chain, Green – Type II Dimer Layers.

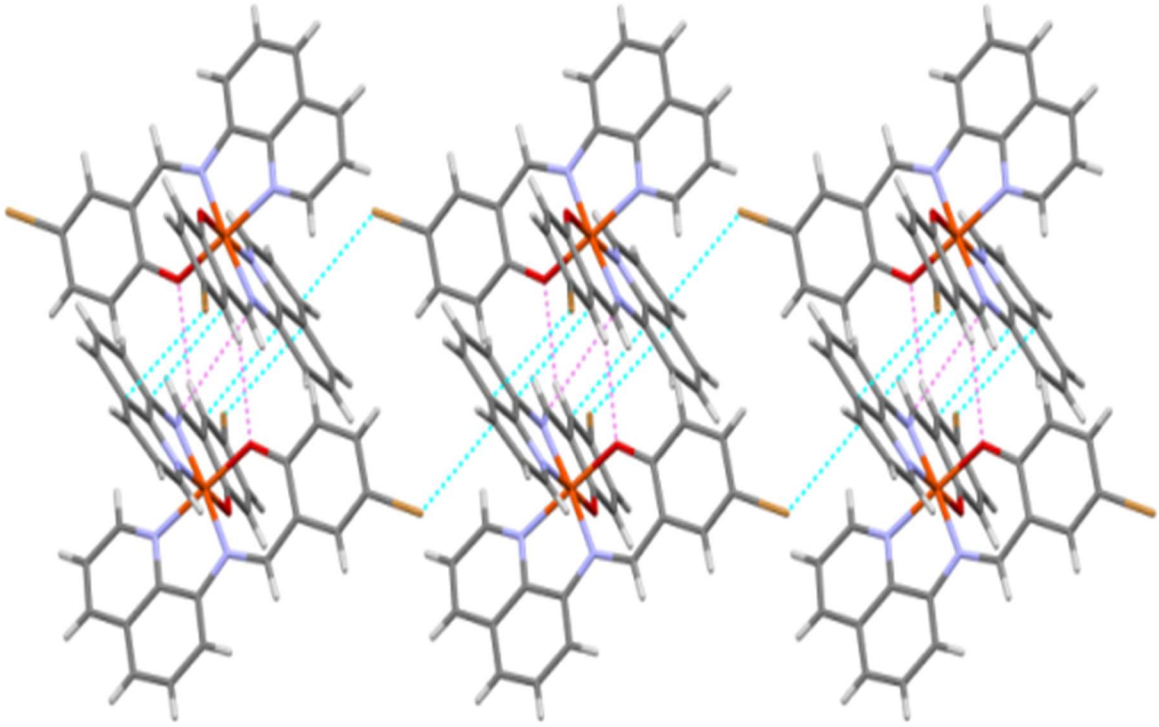

Figure S1: Intrachain arrangements of the cations and DD contacts in the crystal structure of **4.BPh$_4$**. The short contacts colour code corresponds to the difference, Δ in Å, between the distance of the contact and the sum of the van der Waals radii of the involved atoms: violet $\Delta < -0.1$; light blue $\Delta < 0.0$.

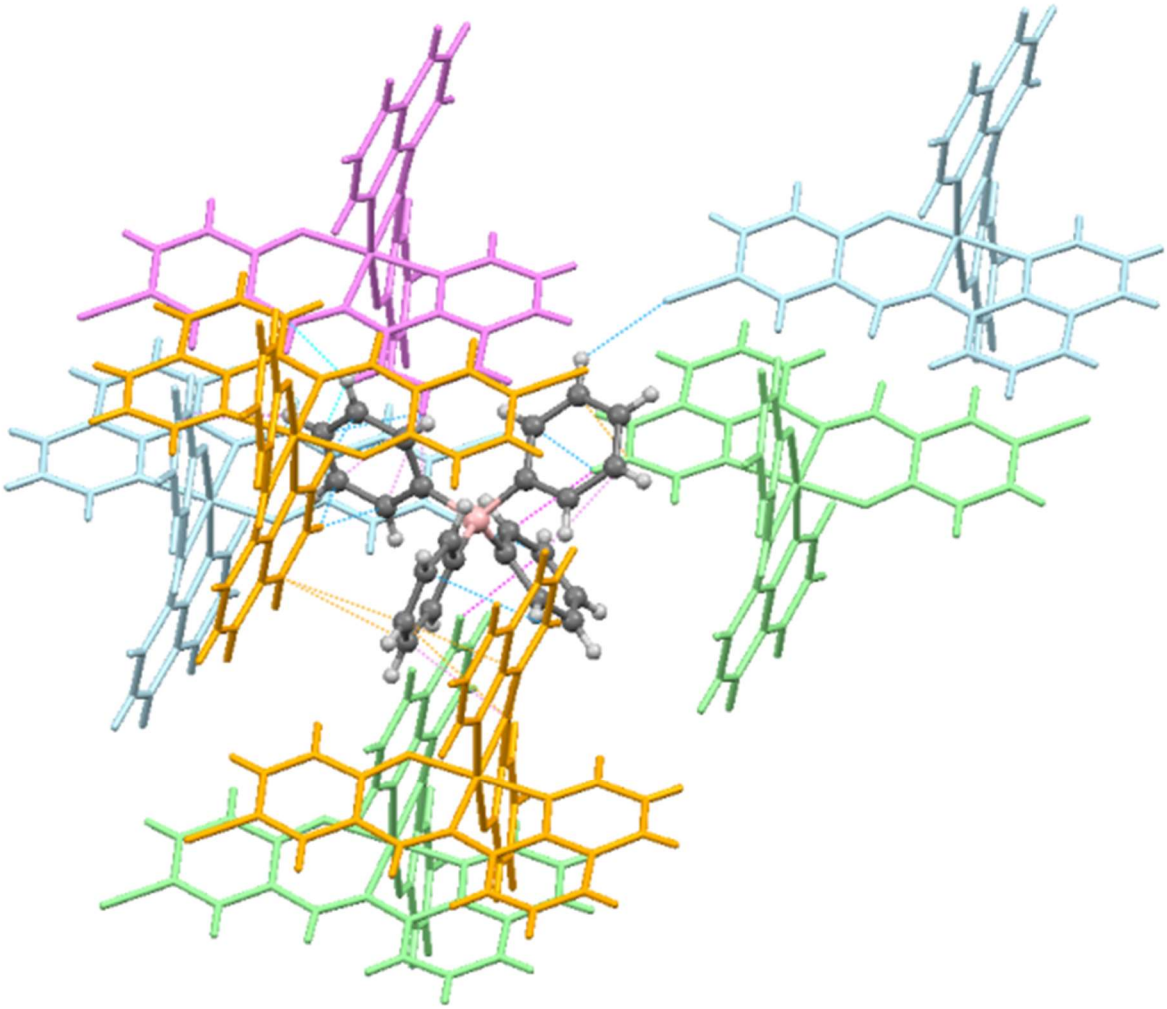

Figure S2: Top view of **4.BPh$_4$** showing the most relevant DA contacts arrangement around one anion with cations from three neighbouring cationic chains. The cations in orange show ππ contacts to the Ph groups of the anion, those in light green show strong CH…π contacts to the anion and the ones depicted in light blue display weaker DA contacts. The short contacts colour code corresponds to the difference, Δ in Å, between the distance of the contact and the sum of the van der Waals radii of the involved atoms: magenta $\Delta < -0.2$; violet $\Delta < -0.1$; light blue $\Delta < 0.0$; orange $\Delta < 0.1$).

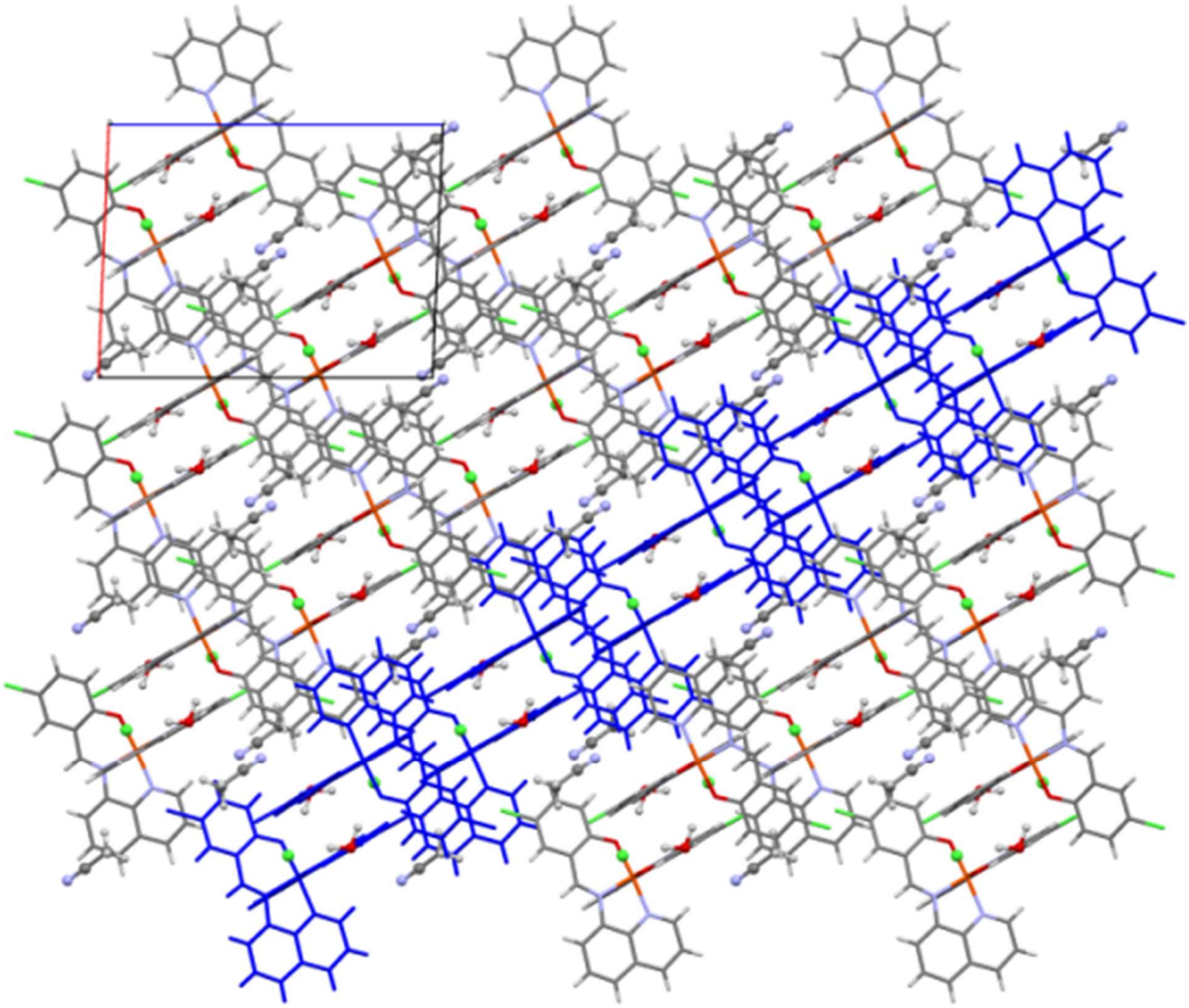

Figure S3: View of the crystal structure of **3.Cl.MeCN.H_2O** along *b*. The cations belonging to one of the cationic layers are depicted in dark blue.

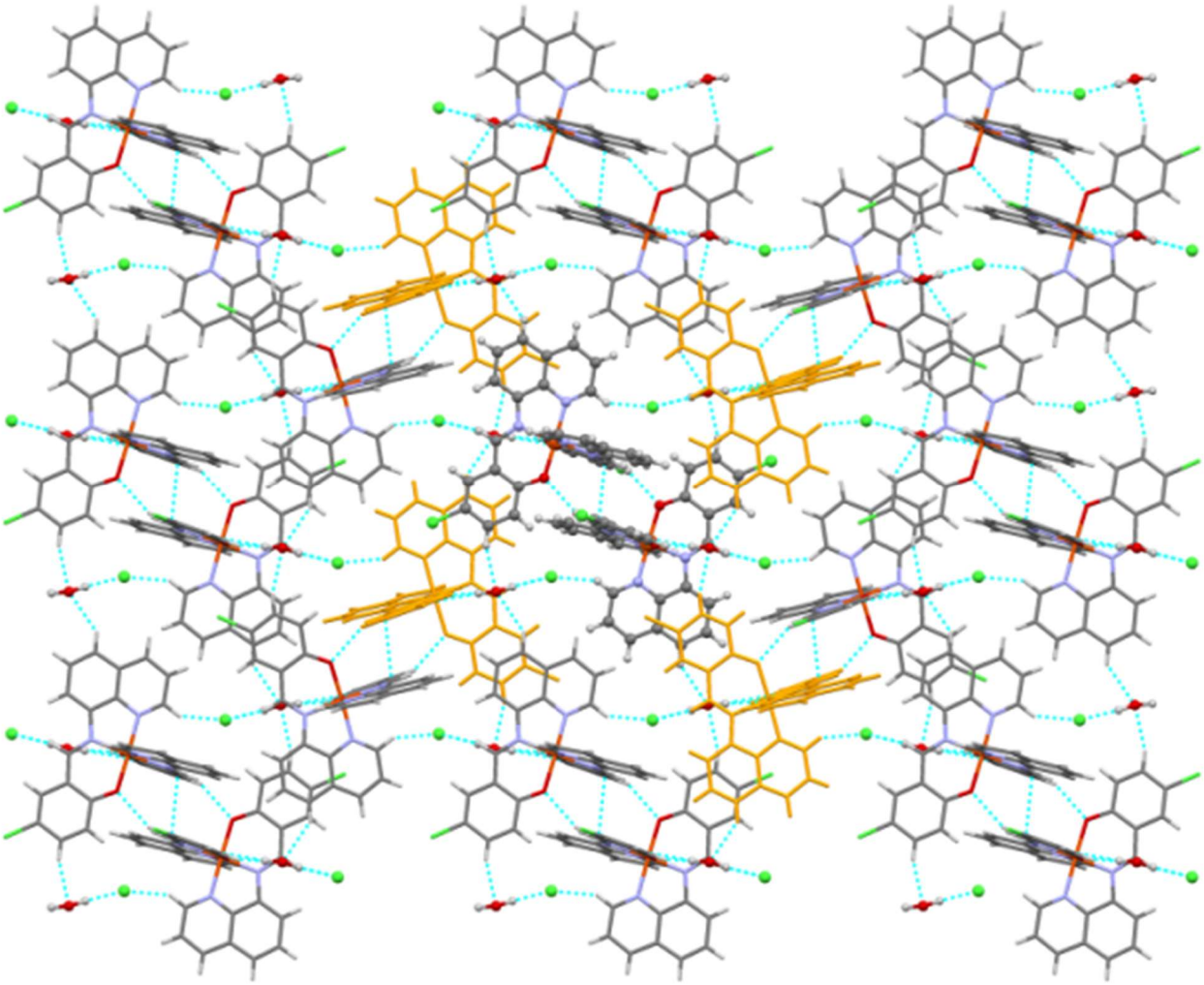

Figure S4: Arrangement of the cations, anions and H_2O molecules within one layer of **3.Cl.MeCN.H_2O** . The four cations in orange show ππ DD interactions with the central cationic dimer. Only contacts shorter than the sum of the van der Waals radii are observed, shown in light blue according to the colour code of the other figures.

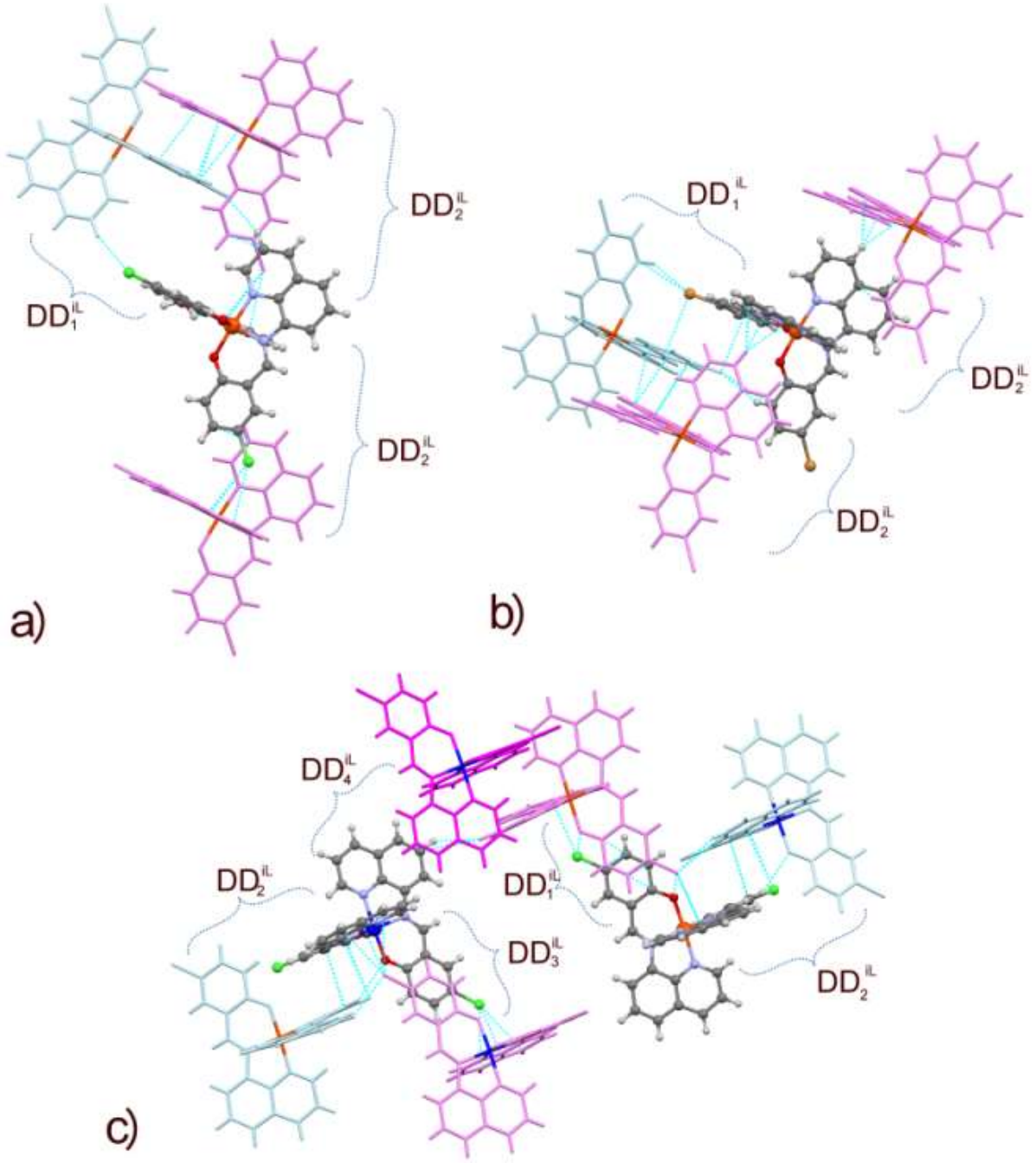

Figure S5: View of the interlayer DD contacts and arrangements of the $[Fe(5\text{-}X\text{-}qsal)_2]+$ cations relative to a central cation (in the default colour scheme) for **3.Cl.MeCN.H_2O** (a), **4.BF_4.H_2O** (b) and **3.ClO_4** (c). Only contacts shorter than the sum of the van der Waals radii are observed, shown in light blue according to the colour code of the other figures.

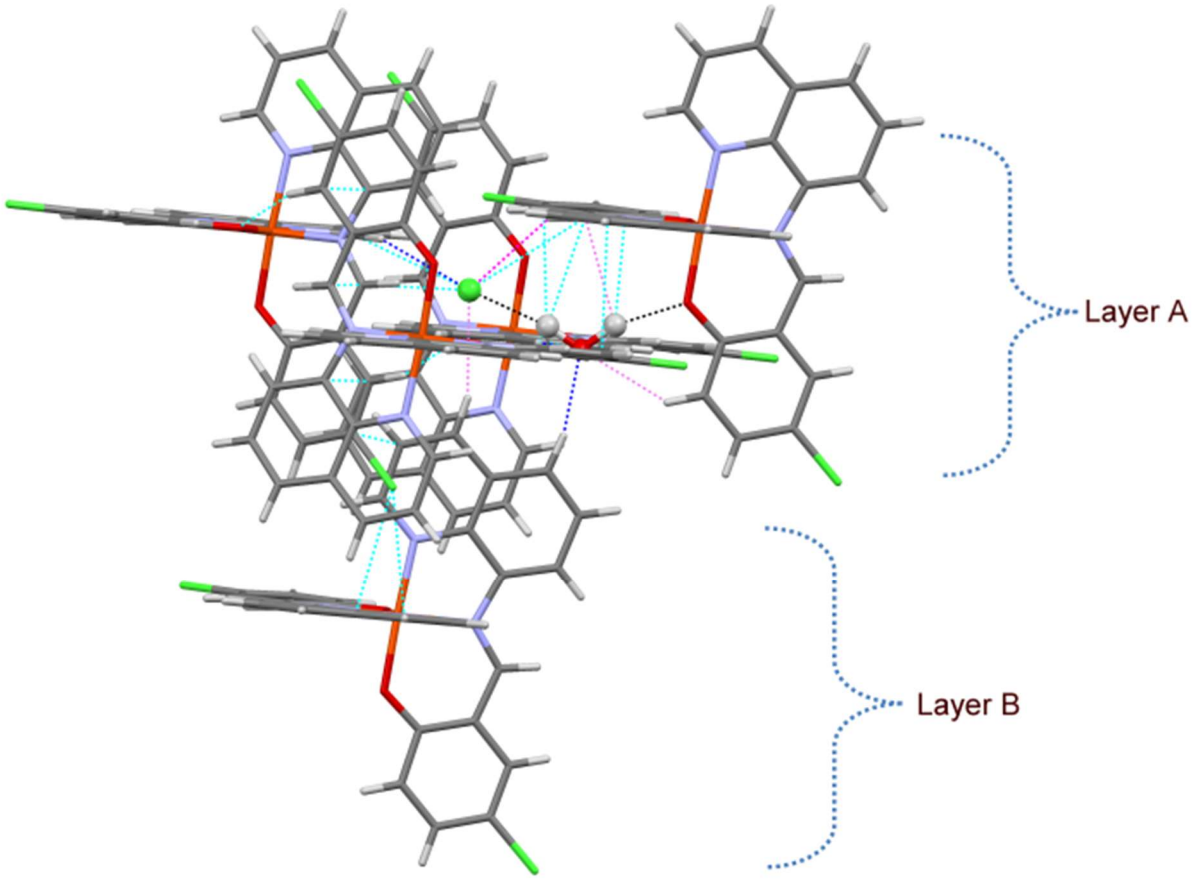

Figure S6: Indirect (D…X…D) connectivity mediated by one strongly coupled $Cl^{-}\cdots H_2O$ pair in **3.Cl·MeCN·H₂O**. The short contacts colour code corresponds to the difference, Δ in Å, between the distance of the contact and the sum of the van der Waals radii of the involved atoms: black $\Delta < -0.5$; dark blue $\Delta < -0.3$, magenta $\Delta < -0.2$; violet $\Delta < -0.1$; light blue $\Delta < 0.0$.

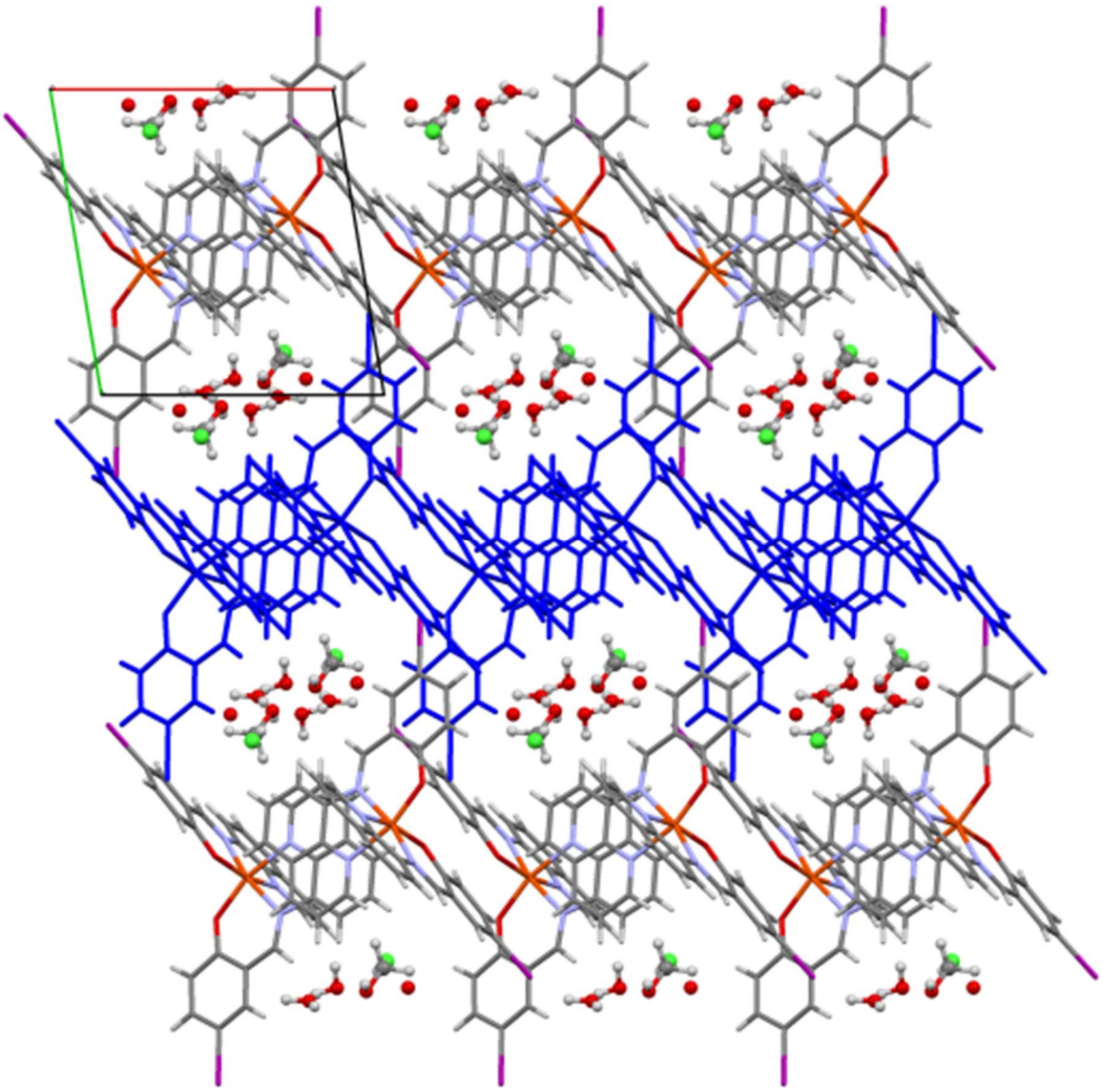

Figure S7: View of the crystal structure of **5.Cl.MeOH.3H$_2$O** along *c*. The cations belonging to one of the cationic layers are depicted in dark blue.

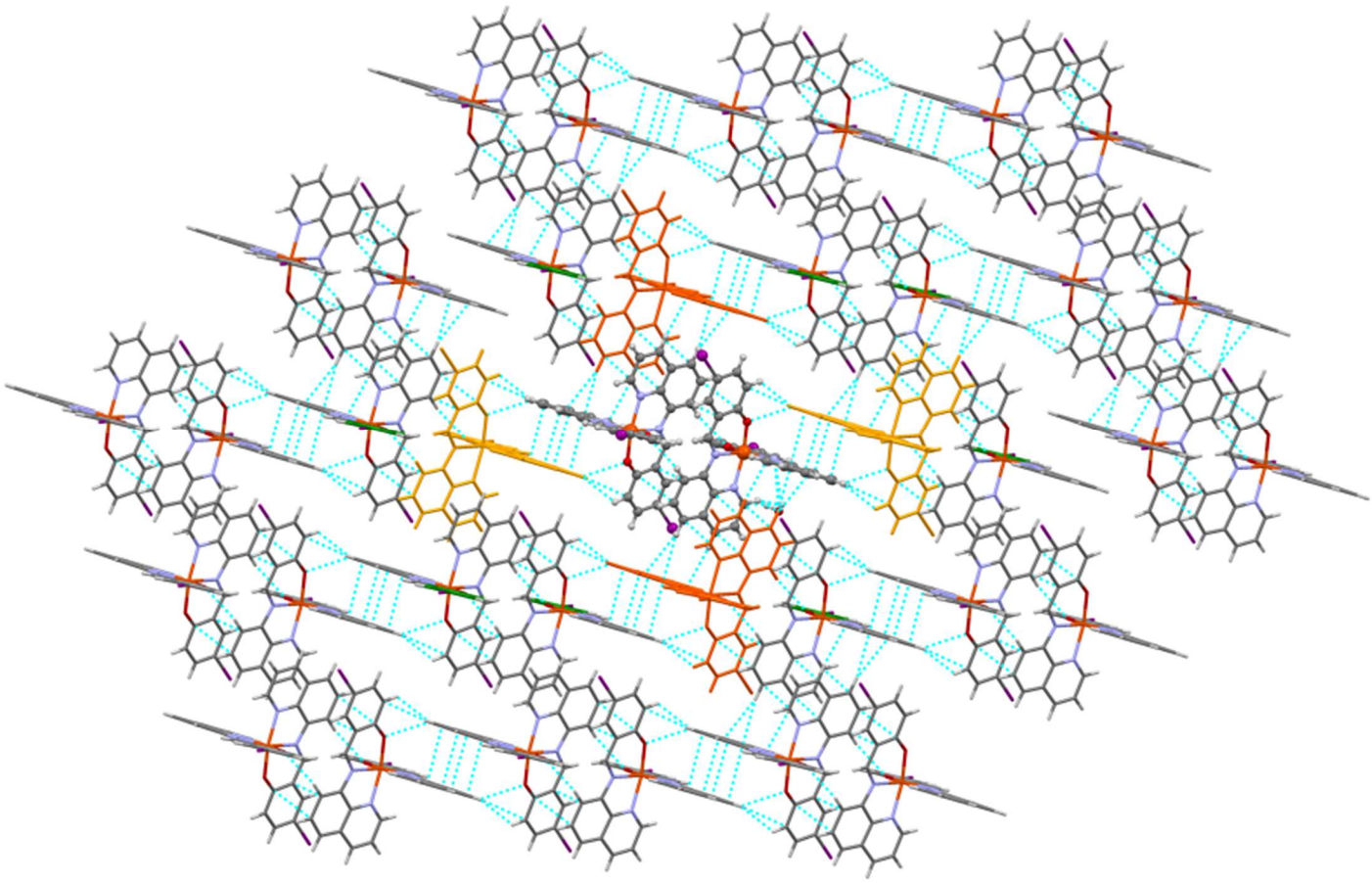

Figure S8: Arrangement of the cations within one layer of **5.Cl.MeOH.3H$_2$O**. The four cations in orange show strong ππ DD interactions with the central cationic dimer. The cations in darker orange correspond to cations with even stronger DD interactions, DD$^{iL}{}_1$, where the ππ interactions are reinforced by strong two fold CH…π interactions. Only contacts shorter than the sum of the van der Waals radii are observed, shown in light blue according to the colour code of the other figures.

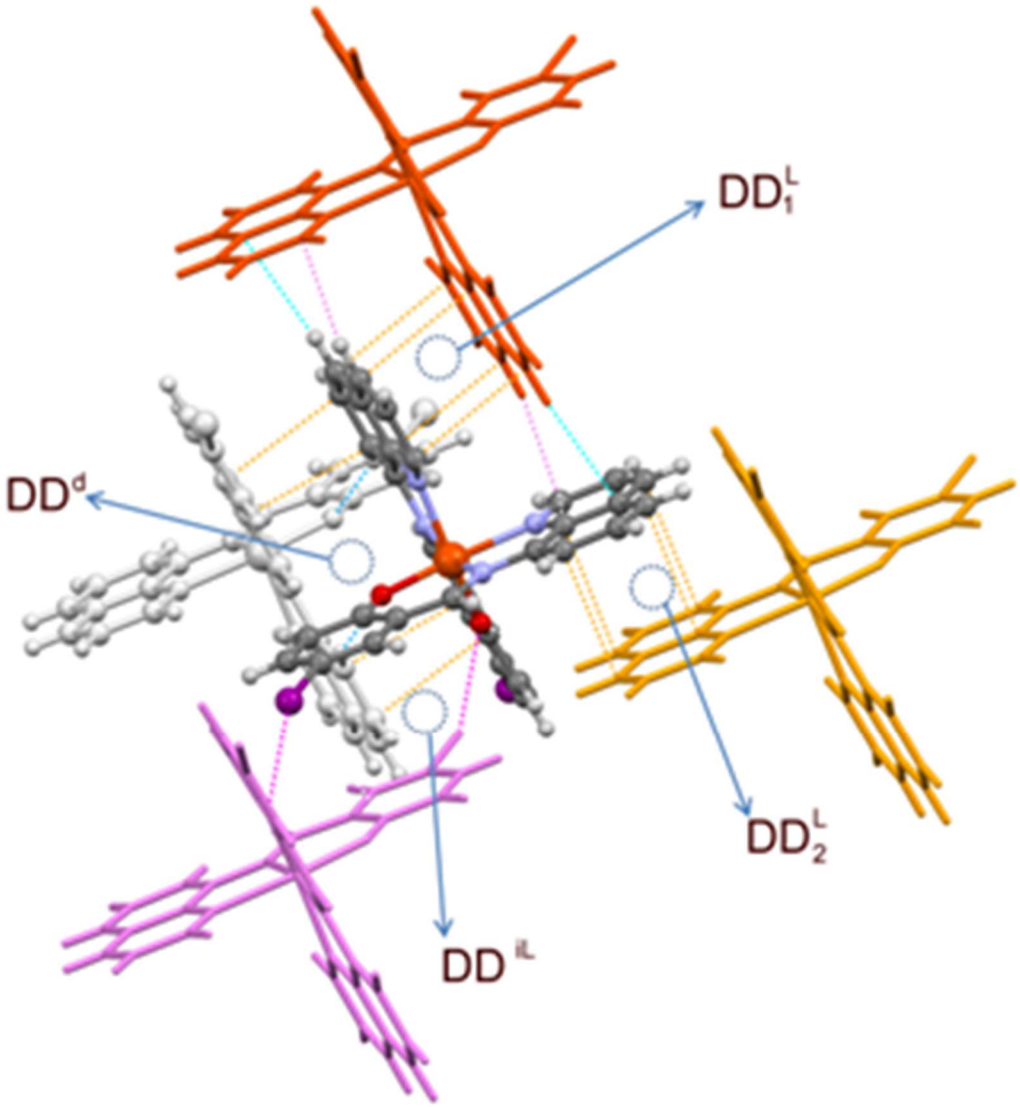

Figure S9: View of the DD contacts and arrangements of the $[Fe(5\text{-I-qsal})_2]^+$ cations relative to a central cation (in the default colour scheme) for **5.Cl.MeOH.3H$_2$O**. The short contacts colour code corresponds to the difference, Δ in Å, between the distance of the contact and the sum of the van der Waals radii of the involved atoms: magenta $\Delta < -0.2$; violet $\Delta < -0.1$; light blue $\Delta < 0.0$; orange $\Delta < 0.1$.

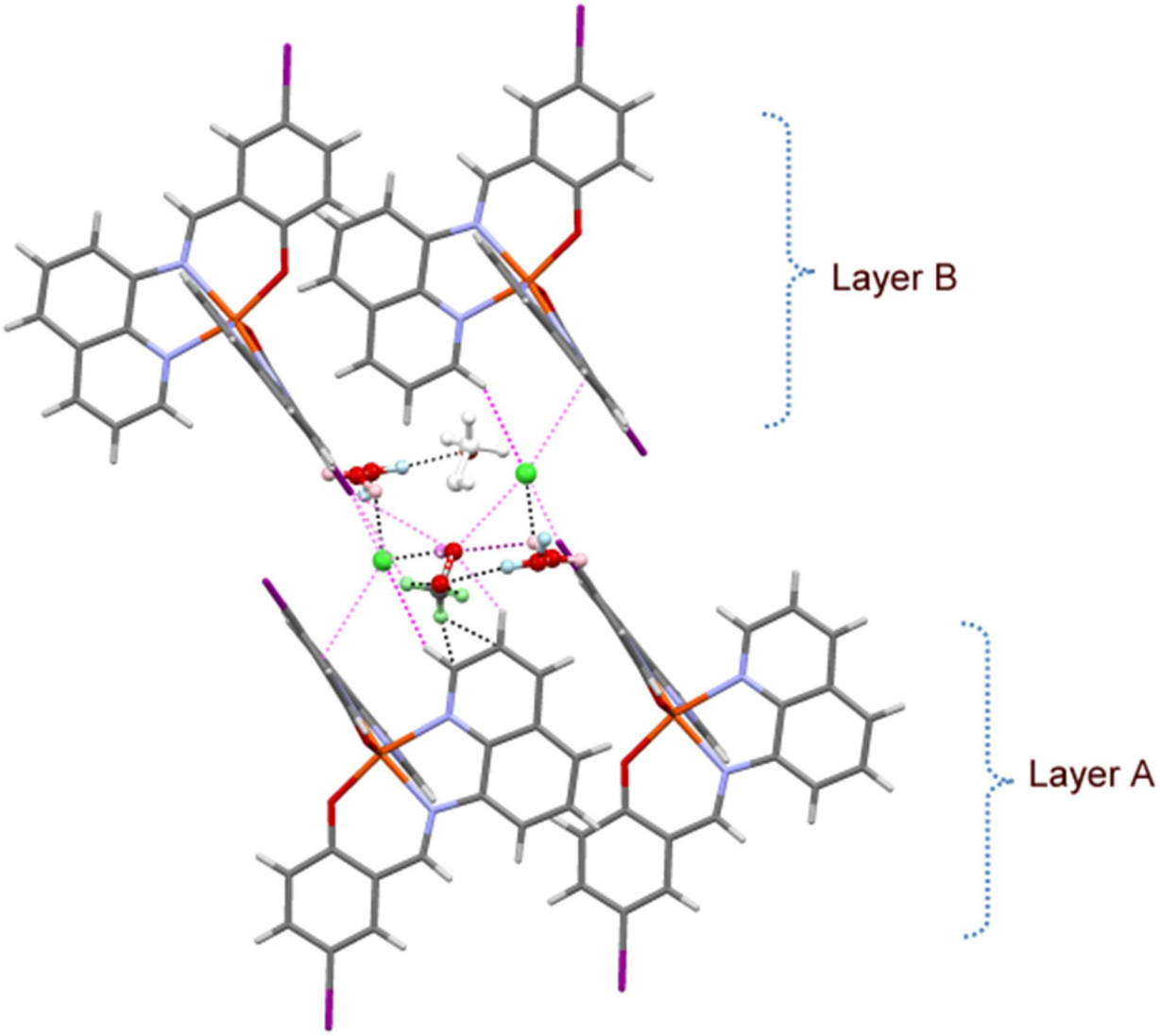

Figure S10: Indirect D…X…D connectivity in **5.Cl.MeOH.3H$_2$O** mediated by strongly coupled aggregates containing two Cl^- anions, six H_2O molecules and one methanol molecule with two possible locations. In one of those locations the MeOH atoms are depicted in light grey and its contacts are omitted. The short contacts colour code corresponds to the difference, Δ in Å, between the distance of the contact and the sum of the van der Waals radii of the involved atoms: black $\Delta < -0.5$; dark blue $\Delta < -0.3$; magenta $\Delta < -0.2$; violet $\Delta < -0.1$.

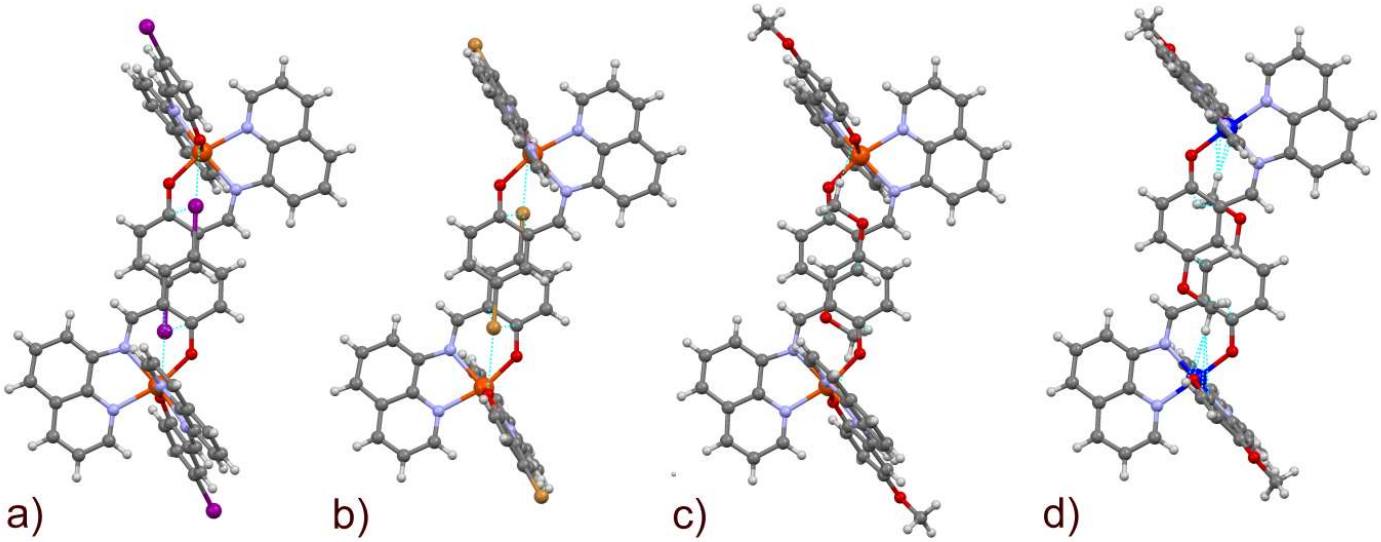

Figure S11: View of the overlaps between the Ph-X groups in the DD interlayer interactions, DD^{iL}, in **5Cl.MeOH.3H$_2$O** (a), **4SCN.0.5H$_2$O** (b), **6Cl.2MeOH.0.5H$_2$O** HS (c) and **6Cl.2MeOH.0.5H$_2$O** LS (d).. View of the overlaps between the Ph-X groups in the DD interlayer interactions, DD^{iL}, in **5Cl.MeOH.3H$_2$O** (a), **4SCN.0.5H$_2$O** (b), **6Cl.2MeOH.0.5H$_2$O** HS (c) and **6Cl.2MeOH.0.5H$_2$O** LS (d). The short contacts colour code corresponds to the difference, Δ in Å, between the distance of the contact and the sum of the van der Waals radii of the involved atoms: violet $\Delta < -0.1$; light blue $\Delta < 0.0$.

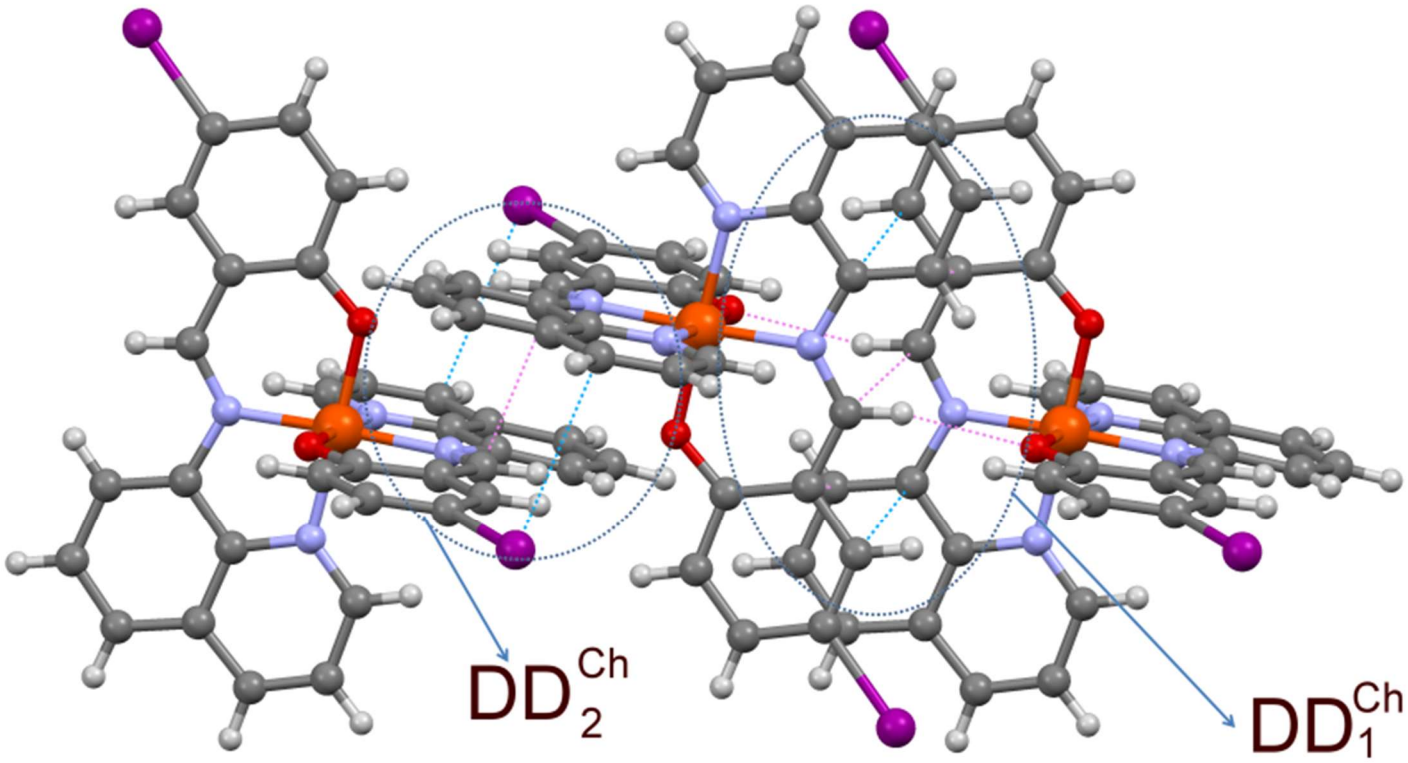

Figure S12: Detail of the intrachain arrangement and the most relevant DD contacts in **5.PF$_6$.1.5H$_2$O**. The short contacts colour code corresponds to the difference, Δ in Å, between the distance of the contact and the sum of the van der Waals radii of the involved atoms: violet $\Delta < -0.1$; light blue $\Delta < 0.0$.

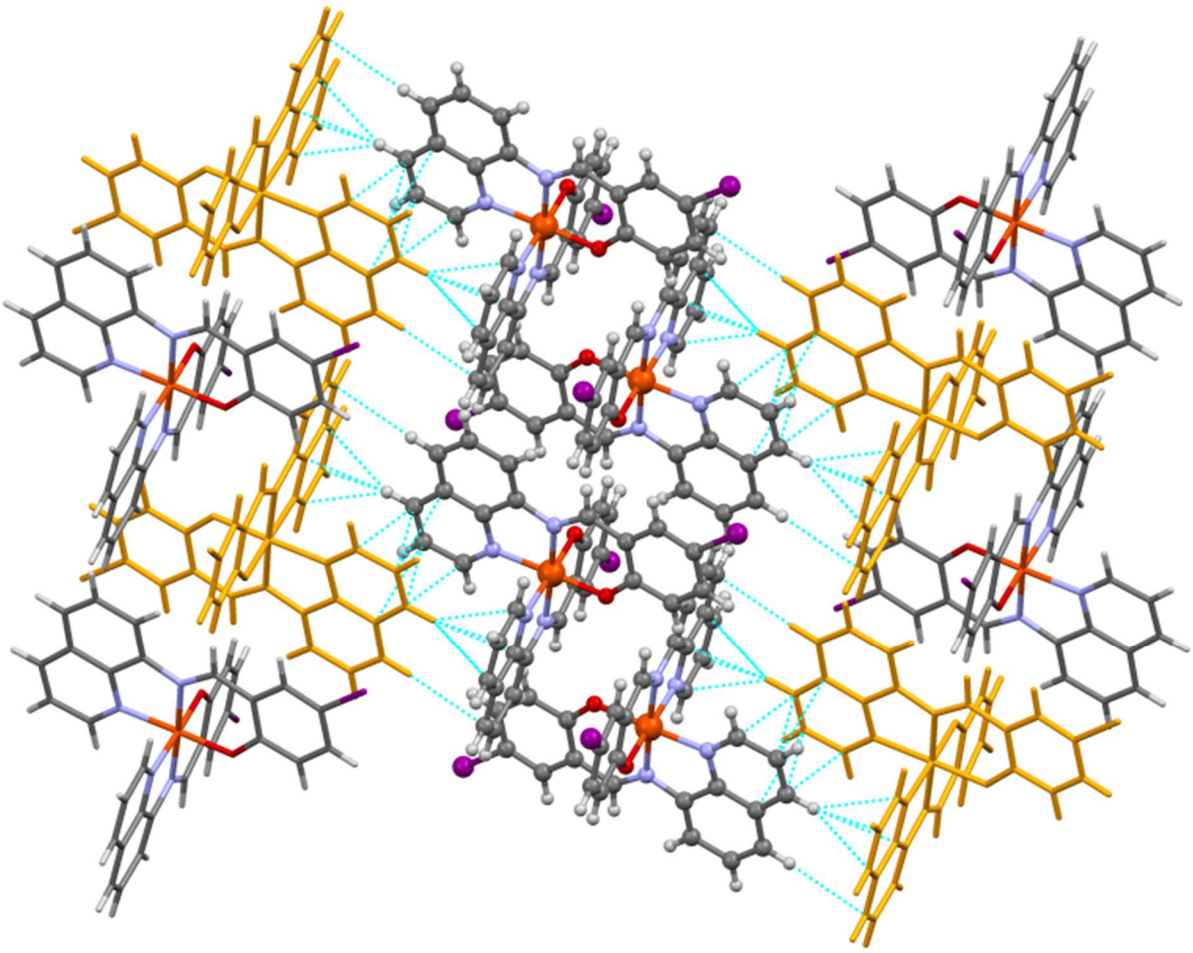

Figure S13: Arrangement of three cationic chains within one layer in **5PF$_6$.1.5H$_2$O**. The cations in central chain are in the "ball and stick mode", while the cations of the other two are represented in the "stick mode". The cations in orange displays strong ππ interactions with cations from the central chain further reinforced by two fold CH…π interactions. Only contacts shorter than the sum of the van der Waals radii are observed, shown in light blue according to the colour code of the other figures.

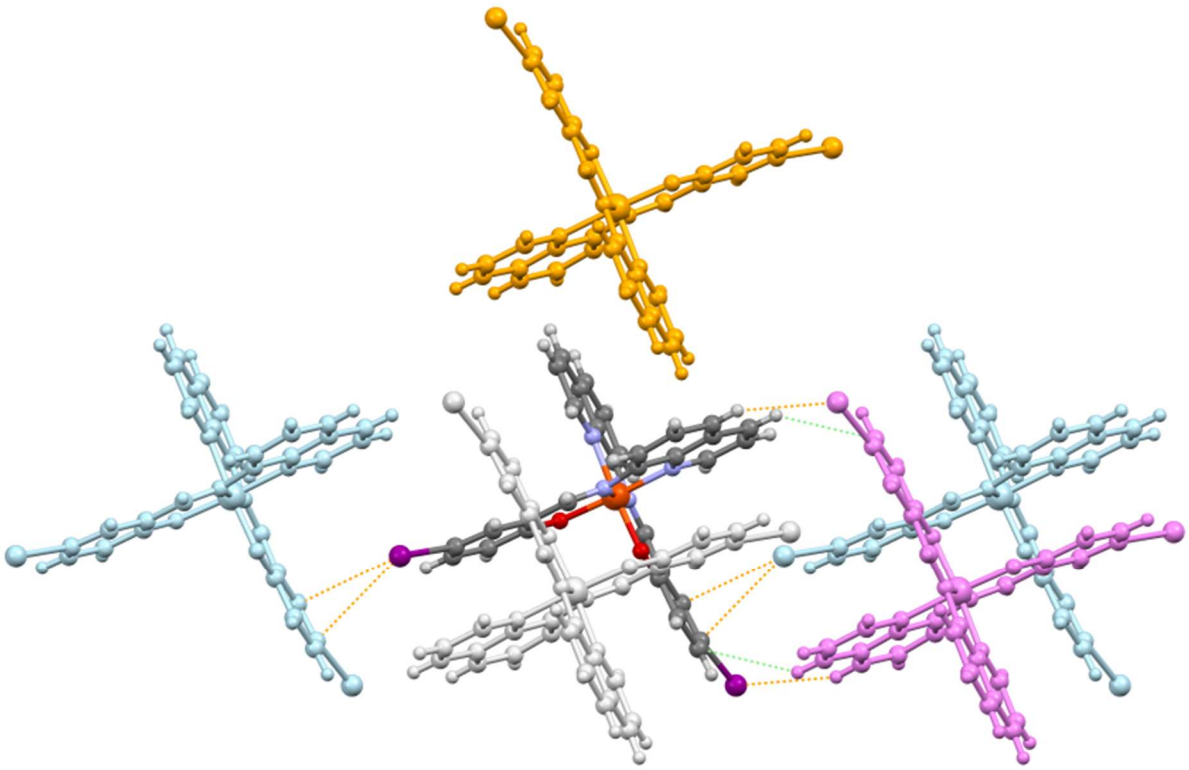

Figure S14: View in the default colour scheme of the interlayer DD contacts and arrangements of the $[Fe(5\text{-I-qsal})_2]^+$ cations relative to a central cation for **5.PF$_6$.1.5H$_2$O**. Only the cations depicted in light blue and in violet belong to the neighbouring layers, those in light grey and orange are located in the same layer as the central cations (the contacts involving these cations are omitted for clarity). The short contacts colour code corresponds to the difference, Δ in Å, between the distance of the contact and the sum of the van der Waals radii of the involved atoms: orange $\Delta < 0.1$; light green $\Delta < 0.2$.

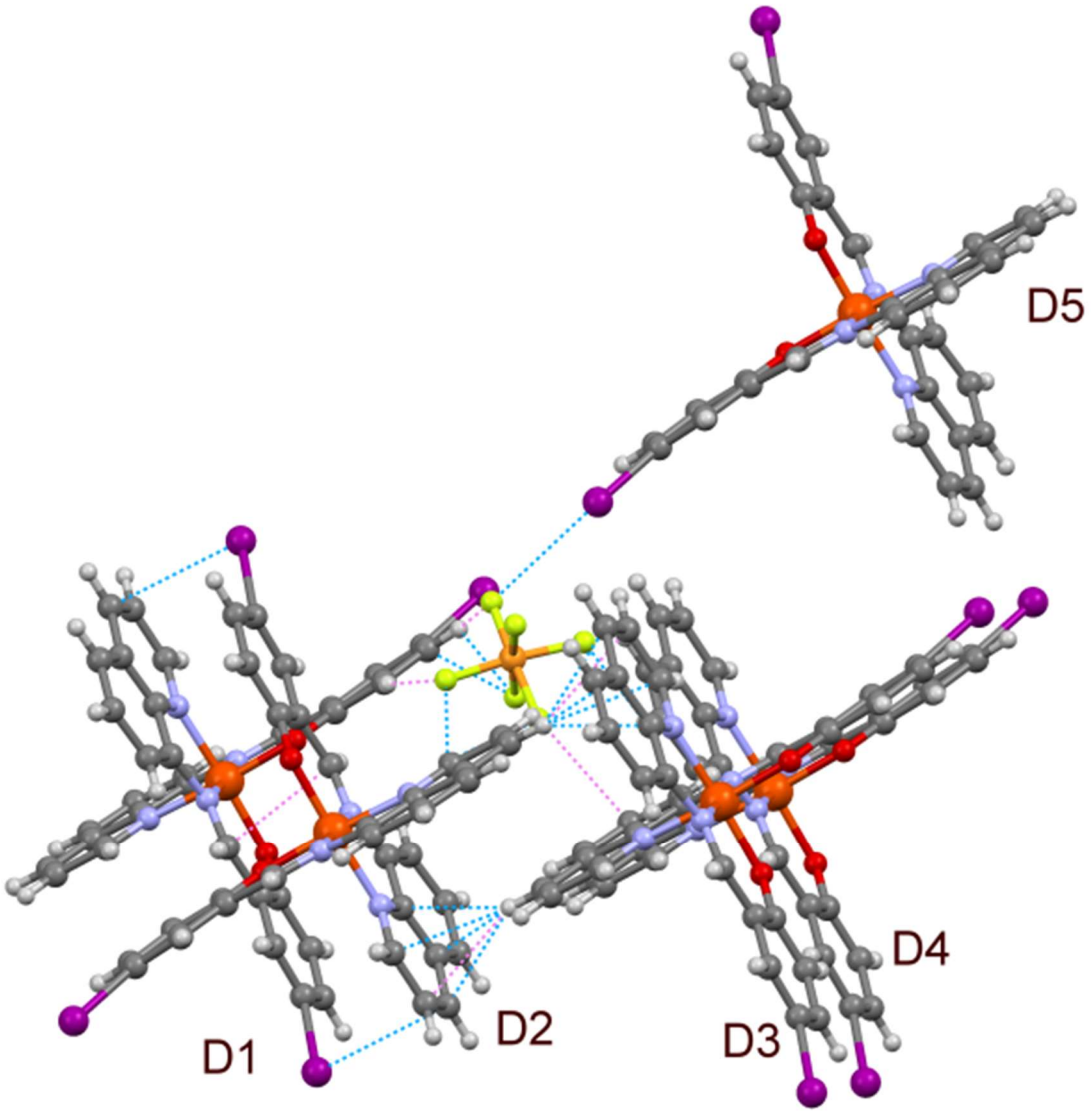

Figure S15: Indirect (D…A…D) connectivity mediated by one PF_6^- anion in **5.PF$_6$.1.5H$_2$O**. The anion shows interactions to four cations (D1-D4) in one layer and to another cation (D5) located in a neighbouring layer. The short contacts colour code corresponds to the difference, Δ in Å, between the distance of the contact and the sum of the van der Waals radii of the involved atoms: violet $\Delta < -0.1$; light blue $\Delta < 0.0$.

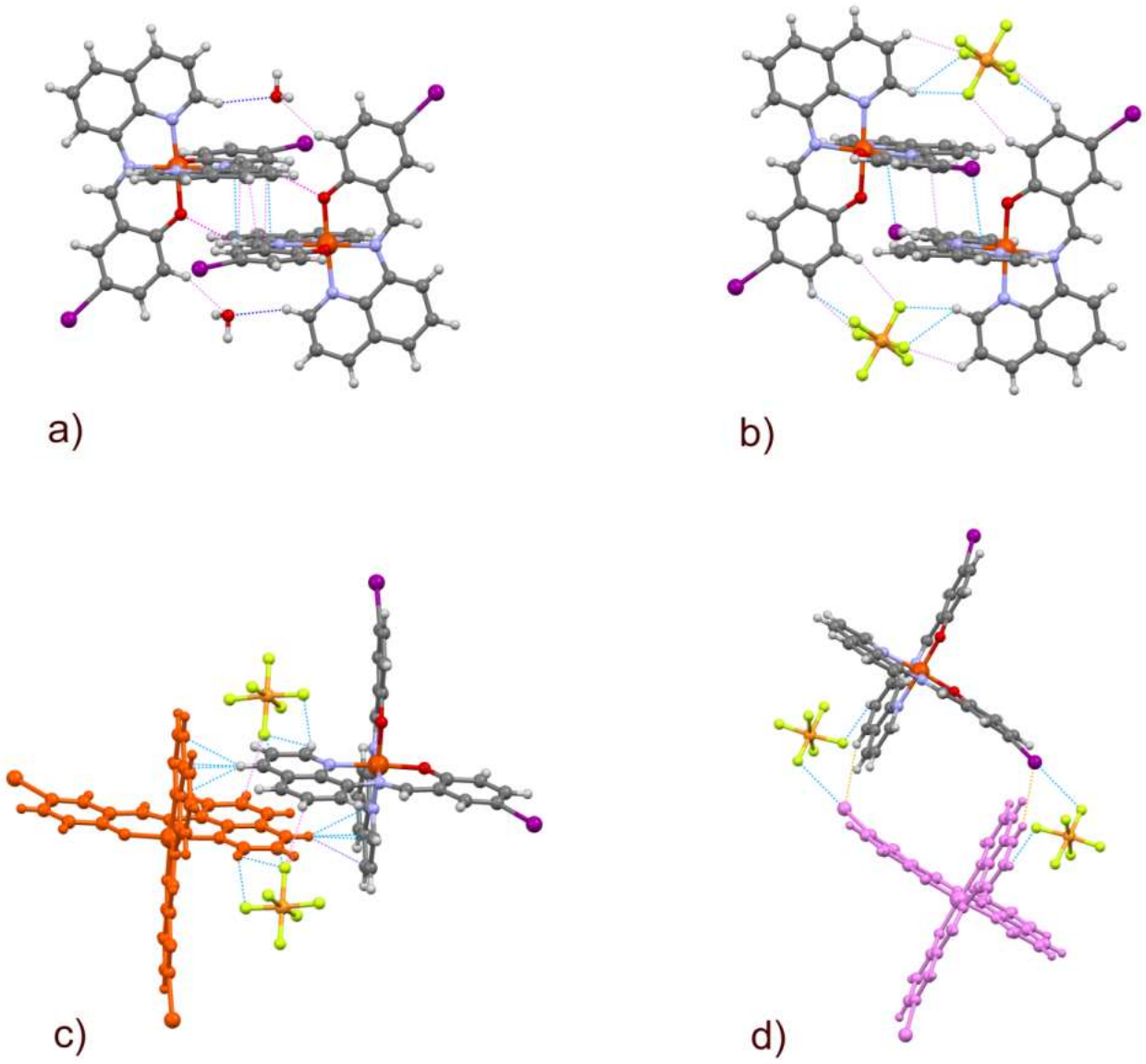

Figure S16: Indirect connectivity assistance to the direct DD intrachain, (a) $DD^{Ch}{}_1$ and (b) $DD^{Ch}{}_2$, intralayer (c) DD^{L} and interlayer (d) $DD^{iL}{}_1$ interactions in **5.PF$_6$.1.5H$_2$O**. $DD^{Ch}{}_1$ is assisted by a pair of interactions mediated by the H_2O molecules and for $DD^{Ch}{}_2$, DD^{L} and $DD^{iL}{}_1$ the DD interactions are assisted by a pair of DAD connections. The short contacts colour code corresponds to the difference, Δ in Å, between the distance of the contact and the sum of the van der Waals radii of the involved atoms: dark blue $\Delta < -0.3$; magenta $\Delta < -0.2$; violet $\Delta < -0.1$; light blue $\Delta < 0.0$; orange $\Delta < 0.1$.

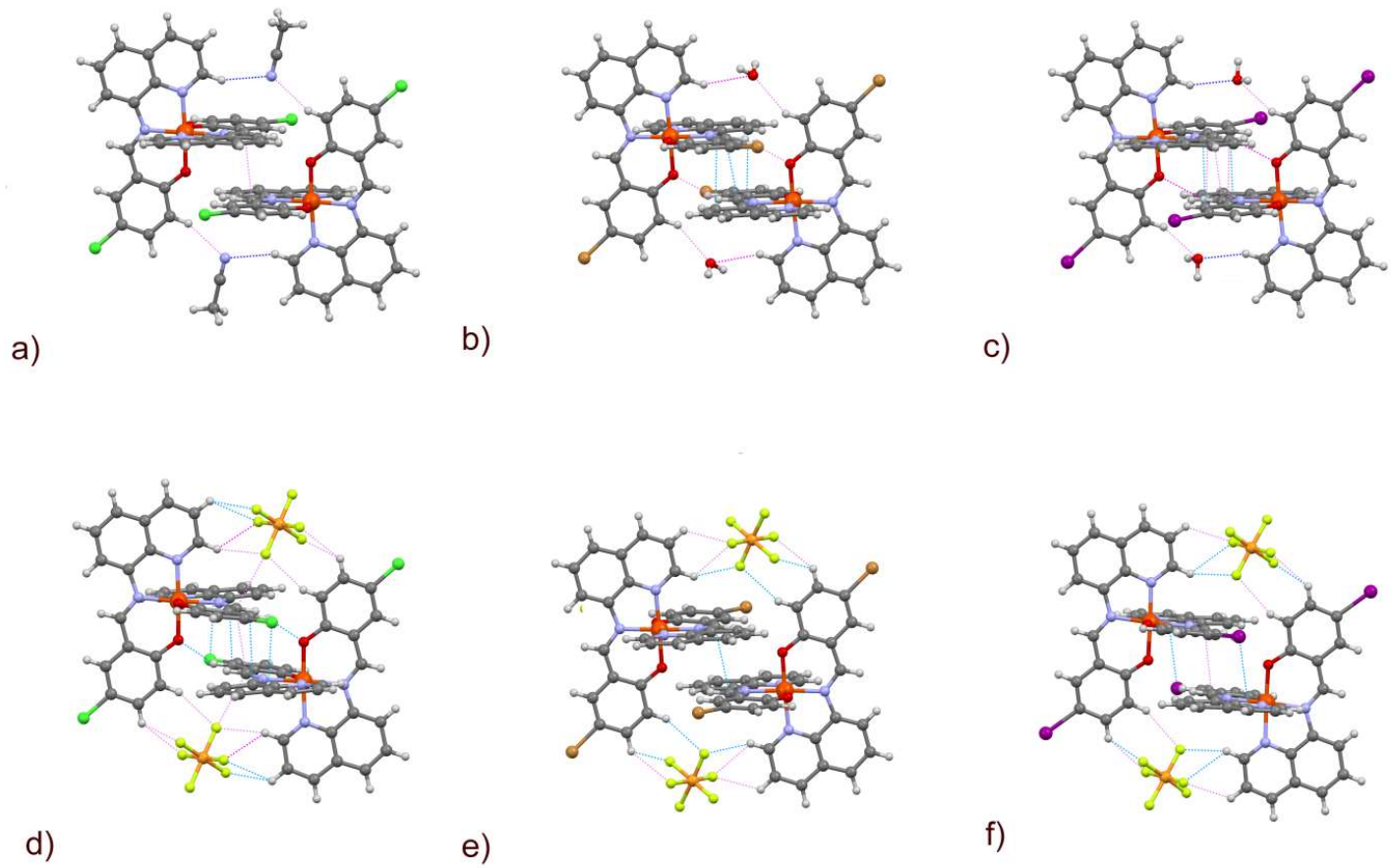

Figure S17: Intrachain indirect connectivity mediated by the solvent molecules and anions to the direct DD interactions (DD^{Ch}_1 and DD^{Ch}_2) in **3.PF$_6$.MeCN** (a and d), **4.PF$_6$.H$_2$O** (b and e) and **5.PF$_6$.1.5H$_2$O** (c and f). The short contacts colour code corresponds to the difference, Δ in Å, between the distance of the contact and the sum of the van der Waals radii of the involved atoms: dark blue $\Delta < -0.3$; magenta $\Delta < -0.2$; violet $\Delta < -0.1$; light blue $\Delta < 0.0$.

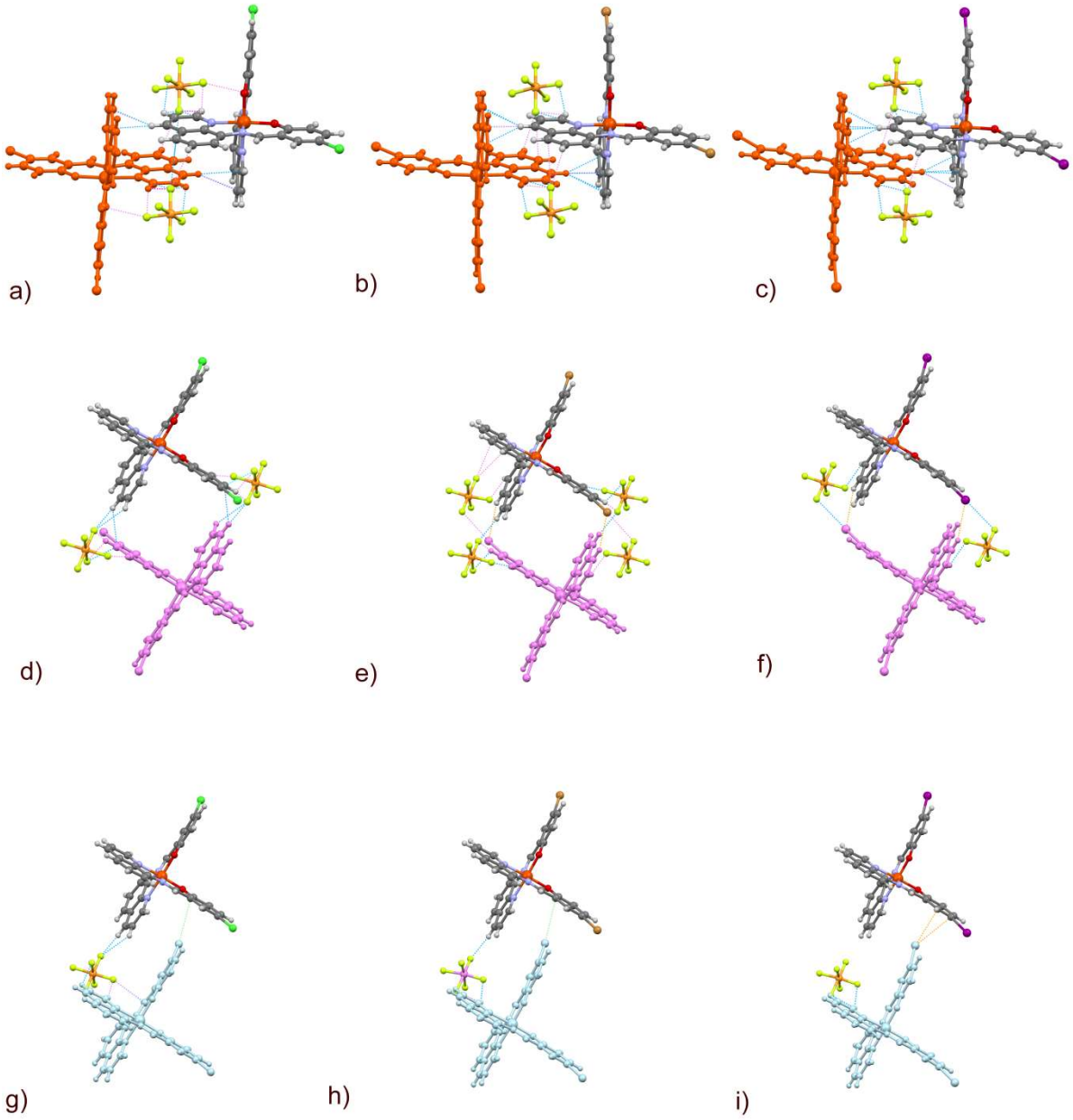

Figure S18: Indirect DAD connectivity assistance to the direct DD intralayer (DD^{L}) and interlayer (DD^{iL}_{1} and DD^{iL}_{2}) interactions regarding **3.PF$_6$.MeCN** (a, d and g), **4.PF$_6$.H$_2$O** (b e and h) and **5.PF$_6$.1.5H$_2$O** (c, f and i). The short contacts colour code corresponds to the difference, Δ in Å, between the distance of the contact and the sum of the van der Waals radii of the involved atoms: violet $\Delta < -0.1$; light blue $\Delta < 0.0$; orange $\Delta < 0.1$.